

# Recent Advances and Applications Toward Emerging Lithium–Sulfur Batteries: Working Principles and Opportunities

Rongyu Deng, Meng Wang, Huanyu Yu, Shunrui Luo, Jinhui Li\*, Fulu Chu, Bin Liu\*, and Feixiang Wu\* 

**Lithium–sulfur (Li–S) batteries have been considered as promising candidates for large-scale high energy density devices due to the potentially high energy density, low cost, and more pronounced ecological compatibility. However, the complex Li–S conversion reactions, unsatisfactory battery performance, and unsafe metallic Li anode restrict the development of Li–S batteries to achieve commercialization. This review mainly focuses on three aspects which are the remaining challenges, recent advances, and applications in Li–S batteries. Firstly, this review portrays Li–S conversion chemistry involving the multi-step and multi-electron reaction mechanism, as well as the remaining challenges. Then, the scientific strategies and very recent advances of the cathode, electrolyte, lithium anode, and other constituent parts of Li–S batteries are detailedly summed up, as well as their advantages and limitations. For the sake of promoting the Li–S batteries practicalization, next section is primarily concerned with problems, the corresponding solutions, and application scenarios of practical pouch cells. Finally, the important findings as guidelines and some future directions as trends for developing emerging Li–S batteries are briefly summarized.**

## 1. Introduction

As the global energy dried up, searching new sources of energy utilization, transformation, and storage system has become an imminent task.<sup>[1,2]</sup> In terms of energy storage fields, most of the market share has

R. Deng, H. Yu, Dr. S. Luo, F. Chu, Prof. F. Wu

School of Metallurgy and Environment, Engineering Research Center of the Ministry of Education for Advanced Battery Materials, Hunan Provincial Key Laboratory of Nonferrous Value-added Metallurgy, Central South University, Changsha 410083, China

E-mail: feixiangwu@csu.edu.cn

M. Wang, Prof. B. Liu

Key Laboratory of Building Safety and Energy Efficiency, Ministry of Education, Department of Water Engineering and Science, College of Civil Engineering, Hunan University, Changsha 410082, China

E-mail: ahxclb@163.com

Prof. J. Li

School of Materials Metallurgy and Chemistry, Jiangxi University of Science and Technology, Ganzhou 341000, China

E-mail: jinhuili@jxust.edu.cn

 The ORCID identification number(s) for the author(s) of this article can be found under <https://doi.org/10.1002/eem2.12257>.

DOI: 10.1002/eem2.12257

been occupied by lithium-ion batteries (LIBs), which have been widely utilized as power supplies in most digital products, electric vehicles, aero crafts, electrical tools, robots, etc. Current commercial LIBs are mainly composed of layered transition metal oxide or lithium iron phosphate cathodes, and graphite anodes. However, these commercial electrode active materials are suffering from the bottleneck of low specific capacities that limit the improvement of energy density level of presented Li-ion batteries. They are almost up to the ceiling. In addition, Ni- and Co-based cathodes with scarce resources are rather expensive and relatively toxic, which restricts the large-scale applications so far. Thus, it is of great significance to develop the next-generation rechargeable batteries with the performance of high specific energy and volumetric energy density, long lifespan, low toxicity, and low cost.<sup>[3–8]</sup>

In such a context, thanks to the potentially high specific energy and low cost, lithium–sulfur batteries have been viewed as one of the most encouraging applicants for next-generation rechargeable battery systems.<sup>[4,9–11]</sup> To be specific, on the one hand, compared with current commercial cathodes, sulfur delivers almost 8–10 times theoretical specific capacity. For another, elemental sulfur is naturally plentiful and environmentally friendly, which fits the future large-scale applications very well. However, the practical applications of Li–S batteries are hindered by its intrinsic troubles. Firstly, naturally insulating S and Li<sub>2</sub>S caused severe kinetic issues of complex conversion reaction processes among sulfides, demonstrating rather poor electrochemical performance: low-capacity utilization and low practical energy density.<sup>[12,13]</sup> Secondly, as intermediate products, the high solubility of long-chain lithium polysulfides (LiPSs) in most organic liquid electrolytes induces the annoying shuttle effects during cycles. The soluble sulfur species shuttled between cathode and anode, which worsen the reaction interface.<sup>[14]</sup> Thirdly, severe volume change (80%) during lithiation resulted in the mechanical properties of sulfur cathodes decline.<sup>[12,15]</sup> For practical applications, key parameters like the composition of battery materials including active mass loading and amount of electrolyte need to be determined.<sup>[16]</sup> In addition, safety issues induced by metallic Li anode and battery management should be carefully considered to guarantee the large-scale adoption of Li–S batteries.<sup>[17]</sup> In the last 10 years, Li–S batteries have been promoted by a mass of research

efforts, aiming to build better Li-S batteries with high specific energy, long lifespan, and high safety. In particular, the current studies focused on inhibiting polysulfide shuttle effects, preventing the growth of Li dendrites, and improving the lithium–sulfur conversion reaction kinetics. Although significant progresses have been made in overcoming basic scientific issues of lithium–sulfur conversion chemistry, there is still a large gap between laboratory investigation and industrial production. In order to promote the commercialization of Li-S batteries, more efforts are needed in material design, structural optimization, and metallic lithium protection under actual working conditions.<sup>[14,16,18]</sup>

This review focuses on the most recent advances and applications toward emerging Li-S batteries. Firstly, the working principle and remaining challenges of Li-S batteries are briefly illustrated. Afterward, we summarize the most recent studies of cathode, electrolyte, lithium anode, and other constituent parts of Li-S batteries separately, mainly including their current advances, corresponding working mechanisms, and limitations. In order to understand and promote the commercialization of Li-S batteries, practical issues, potential solutions, and application scenarios of practical pouch cells are also discussed in detail. Finally, we review the recent research findings involved each part of Li-S batteries and propose several directions as guidelines and trends for achieving major breakthroughs and practical applications in the near future.

## 2. Li-S Conversion Chemistry

The diagrammatic sketch and reaction mechanism of Li-S batteries are shown in **Figure 1**. Since sulfur atoms are the active redox centers in the cathode materials, the Li-S conversion reaction involving multi-steps and two-electron transfer takes place during charging and discharging, which is different from the traditional Li-ion battery based on

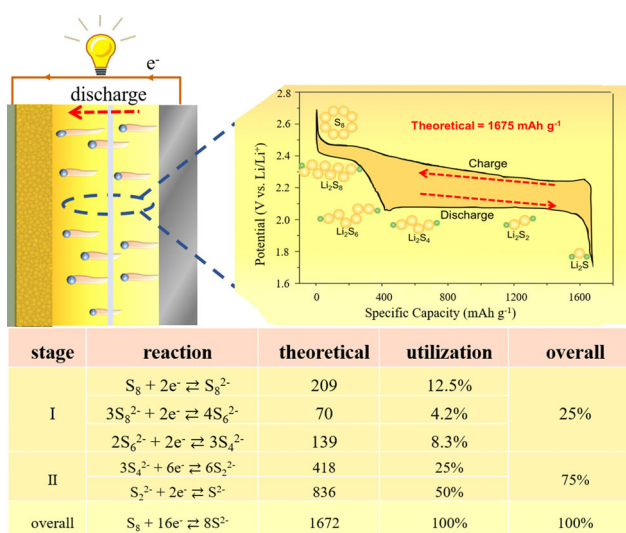


**Figure 1.** The diagrammatic sketch and reaction mechanism of Li-S batteries. Adapted with permission.<sup>[7]</sup> Copyright 2021, American Chemical Society.



**Rongyu Deng** obtained his Bachelor degree from Central South University in 2020. Now, he is pursuing his Ph.D. degree under the supervision of Prof. Feixiang Wu at the School of Metallurgy and Environment, Central South University. His current research interests mainly focus on the electrolyte and metal anodes for high-energy rechargeable batteries.



**Meng Wang** is currently studying for her Master degree under the guidance of Assistant Professor Bin Liu from the School of Civil Engineering of Hunan University. She received her Bachelor degree from Zhengzhou University in 2019. Her current research focuses on lithium–sulfur battery electrolytes.



**Huanyu Yu** is currently pursuing his Master degree under the supervision of Prof. Feixiang Wu in the School of Metallurgy and Environment, Central South University (CSU). He obtained his Bachelor degree from Jiangxi University of Science and Technology (JUST) in 2019. His current research interests mainly focus on the design of cathode materials for high specific energy lithium–sulfur batteries.



**Shunrui Luo** is a postdoctoral fellow in the group of Dr. Feixiang Wu in Central South University performing optimization metal fluorides-based composites as cathodes for Li-ion batteries. She obtained her Ph.D. degree from Chemistry and Chemical Engineering, Chongqing University in 2020. Her research interests are in the areas of synthesis, mechanism, and structure–property relationship of shape-controlled nano- and micromaterials.

one-electron transfer cathode materials. Multi-step reaction means that the process involves several chemical reaction steps and multiple phase transitions. The typical galvanostatic discharge curve of the Li-S battery is composed of two plateaus including a high voltage about 2.3 V plateau and a low plateau about 2.1 V,<sup>[18]</sup> which correspond to two main reaction processes of lithium–sulfur batteries. The 2.3 V plateau indicates the lithiation of S<sub>8</sub> to long-chain polysulfides in the order of S<sub>8</sub>-Li<sub>2</sub>S<sub>8</sub>-Li<sub>2</sub>S<sub>6</sub>-Li<sub>2</sub>S<sub>4</sub>, contributing 25% of the specific capacity about 418 mAh g<sup>-1</sup>. The low voltage plateau is the consequence of the phase transitions from Li<sub>2</sub>S<sub>4</sub> to Li<sub>2</sub>S<sub>2</sub>, and then to Li<sub>2</sub>S, attributing to 75% of the specific capacity about 1254 mAh g<sup>-1</sup>. Specifically, as shown in Figure 1, S<sub>8</sub> molecule captures two electrons and turns itself into S<sub>8</sub><sup>2-</sup>, and then S<sub>8</sub><sup>2-</sup> gradually catches electrons and becomes several different polysulfides until it becomes S<sup>2-</sup> and the reaction ends. Overall, 16 electrons will be consumed if S<sub>8</sub> molecule completely changes into Li<sub>2</sub>S. As early as 1962, Herbet and Ulam firstly used sulfur as cathode material and proposed the electrochemical reaction equation: 2Li + S ↔ Li<sub>2</sub>S. Studies just simply mechanically mixed elemental sulfur, conductive agent, and binder. However, sulfur and lithium sulfides (Li<sub>2</sub>S, Li<sub>2</sub>S<sub>2</sub>) with poor electronic conductivity cause rather poor capacity utilizations.<sup>[19]</sup> Furthermore, the soluble lithium polysulfides (LiPSs) (Li<sub>2</sub>S<sub>n</sub>, 2 ≤ n ≤ 8) as intermediate products were undoubtedly produced during discharge processes, LiPSs inevitably shuttled between the cathode and anode, leading to the so-called “shuttle effect.” The dissolution and shuttling of long-chain polysulfides are the main reasons for low utilization of sulfur, poor Coulombic efficiency, and rapid capacity decay.

In summary, on account of the complex chemical react ions and distinctive curves, there are still several major scientific challenges that urgently need to be conquered: 1) thanks to the sulfur molecules dissolve in the ether solvent and open the ring, the first plateau demonstrates excellent reaction kinetics, while concomitantly producing long-chain lithium polysulfides that shuttle between the two electrodes,<sup>[20]</sup> thus generating a series of problems including the occurrence of side reaction, the increase of electrolyte viscosity, the formation of dead sulfur; 2) most of the capacity contribution comes from the second plateau, where involves two chemical reactions, one is Li<sub>2</sub>S<sub>4</sub> transform into Li<sub>2</sub>S<sub>2</sub>, and the other is Li<sub>2</sub>S<sub>2</sub> to Li<sub>2</sub>S. The latter is a transformation reaction between two poorly conductive solid phases, which not only results in greater polarization but also increases the activation energy of the reaction further slows down the kinetics, as can be evidenced by the sharp spike at the front of charge curve where Li<sub>2</sub>S releases the lithium ion.

### 3. Recent Progress of Sulfur Cathode

Currently, the above-mentioned challenges hinder the commercial applications of lithium–sulfur batteries. In order to solve these issues, researchers have made many efforts for Li-S batteries. The most common method to improve the performance of Li-S batteries is to combine conductive carbon materials with active sulfur to form composite materials. Therefore, the introductions of various types of conductive materials such as carbon-based materials,<sup>[21]</sup> polymers,<sup>[22]</sup> polar inorganic materials,<sup>[23,24]</sup> and other polar materials<sup>[25]</sup> into the design of sulfur cathodes are a kind of attractive method to improve the



**Jinhui Li** is a Distinguished Professor Program of Jinggang Scholars in institutions of higher learning, Jiangxi Province, and working in Jiangxi University of Science and Technology. His research focuses on extraction of valuable metals from waste, separation of different metals from multi-metals solution, and recycling and utilization of new energy

materials. He has published over 30 peer-reviewed articles and 4 books, and funded by National Natural Science Foundation (51974140, 52064018), the National Key R&D Program of China, Key Projects of Jiangxi Key R&D Plan (No. 20192ACB70017), and the cultivation project of the State key Laboratory of Green Development and High-value Utilization of Ionic Rare Earth Resources in Jiangxi Province (20194AFD44003).



**Fulu Chu** gained his Bachelor and Master degrees from Xiangtan University in the School of Materials Science and Engineering in 2015 and 2018, respectively. He is currently a Ph.D. candidate in Metallurgical Engineering at Central South University under the supervision of Prof. Feixiang Wu. And during his Master degree, he was a joint-training student under the supervision of Prof. Chilin Li in Shanghai Institute of Ceramics, Chinese Academy of Sciences. His current research interests mainly focus on the interface between Li and liquid electrolyte, dendrite suppression of Li metal anodes, and advanced energy storage/conversion materials.



**Bin Liu** is an assistant professor in the Department of Water Engineering and Science, Hunan University. He did his Ph.D. in Municipal Engineering in 2018 at Harbin institute of technology ( HIT ) and in Chemical Engineering in 2021 at KU Leuven ( KUL ). He has published over 30 peer-reviewed articles with more than 700 citations. His research interests focus on environment chemistry and environmental functional materials.

conductivity of sulfur cathodes and the ability of trapping active sulfur species. In addition, these conductive host materials can alleviate the shuttle of intermediate LiPSs by physical and chemical confinement, improving the cycle stability and specific capacity of Li-S batteries.

### 3.1. Carbon Material Host

Due to their high surface area, excellent mechanical stability, tunable structure, and excellent conductivity, carbon materials are widely used as sulfur host materials to confine polysulfides into the porous structures, enhancing the specific capacity utilization of sulfur and resulting in suppressed polysulfide shuttling effects.<sup>[26–31]</sup> Carbon-based materials employed as a sulfur host, including porous carbon, graphene, and carbon nanotubes/fibers greatly improved the electrical conductivity of sulfur cathode as well as immobilized the dissolution of long-chain polysulfide from the cathode into the electrolyte.

Porous carbon-based materials are generally employed as a conductive skeleton to the sulfur cathode, in which polysulfides can be confined in the pores. Due to the wonderful conductivity, high specific surface area, and sufficient pore volume, porous carbon-based materials as sulfur host materials have been largely employed. Simultaneously, the porous structure can effectively buffer the volume expansion caused by the sulfur cathode during discharge. According to different pore sizes, porous carbon materials can be divided into three main categories: 1) microporous carbon (pore size  $<2$  nm), which has been considered as an ideal host material for alleviating the dissolution of long-chain polysulfides due to its size, is similar with that of polysulfides;<sup>[32]</sup> 2) mesoporous carbons (pore sizes 2–50 nm), which have many advantages as sulfur host materials including more available transfer channels for lithium-ion transport, enabling sufficient contact with the electrolyte,<sup>[33]</sup> and increasing sulfur loading in the cathode; 3) macroporous materials (pore sizes  $>50$  nm) are rarely used as sulfur host materials because their pore size is too large to confine sulfur species. Consequently, microporous carbon and mesoporous carbon are universally used as host materials or conductive frameworks in Li-S batteries.

Microporous carbon materials are widely used in the design of Li-S cathodes because their pore sizes are small enough to homogeneously entrap the sulfur intermediates. In the early years, Guo et al. chose microporous carbon (0.5 nm) as a sulfur host. The small sulfur molecules ( $S_{2-4}$ ) were successfully confined into carbon micropores. During discharging and charging, they cannot return to the ring state ( $S_8$ ), thus avoiding the problem of intermediate polysulfides dissolution in electrolyte and suppressing capacity decay in cycles. Consequently, the small sulfur molecules employed as cathode exhibited long-term cycling stability at 0.1 C, where the capacity retention was ~96% after 200 cycles.<sup>[32]</sup> However, in general, microporous carbons as sulfur matrix have the intrinsic disadvantage of low utilization of sulfur species due to limited electrolyte access through small pores, which hinder their widespread development and application. Mesoporous carbon materials have been widely developed to contain sulfur as much as possible in the host materials. In 2009, Nazar and her colleagues made a breakthrough that a highly ordered mesoporous CMK-3 material composed of many hollow carbon rods was reported.<sup>[21]</sup> Sulfur was melted into the voids of CMK-3 at 150 °C by melt-diffusion method. As a result, lithium polysulfides could be physically trapped by pores in conductive CMK-3 mesoporous carbon, achieving a high specific capacity of 1005 mAh g<sup>-1</sup> at 0.1 C. Unfortunately, purely physical adsorption



**Feixiang Wu** is a professor of the School of Metallurgy and Environment at the Central South University (CSU). He did his Ph.D. in Metallurgical Physics and Chemistry in 2014 at CSU. From 2012 to 2014, he was a visiting scholar in Prof. Yushin's laboratory in Materials Science at the Georgia Institute of Technology (GT). After graduation, he worked as a research associate in Yushin group at GT (2015–2016). From 2016 to 2019, he worked as a Humboldt Fellow in Maier group at the Max Planck Institute for Solid-State Research. His research interests focus on electrode materials and electrolytes for rechargeable batteries.

is insufficient to limit the diffusion of polysulfides out of the porous network. Because inherently nonpolar carbons are unfavorable to adsorb the intrinsic polar soluble polysulfides. To further restrain polysulfide shuttle, Nazar et al.<sup>[21]</sup> functionalized the surfaces of carbon-sulfur composites using polyethylene glycol (PEG). The as-prepared electrode materials obtained an ultra-high specific capacity of 1320 mAh g<sup>-1</sup>. This work has a huge boost to the subsequent application of carbon-based materials in cathodes for Li-S batteries. In subsequent investigations, Yang et al.<sup>[34]</sup> reported a novel approach to functionalize mesoporous carbon, which introduced the thiol groups(-SH) into the surface of the mesoporous carbon via a one-polar reaction. This strategy improved not only the conductivity of mesoporous carbon but also the chemical bonding between functional surface and polysulfides, which improved the utilization of sulfur and cycle stability. The original electrode displayed a capacity retention of only 56% after 180 cycles at 0.25 C at a high sulfur loading of 4 mg cm<sup>-2</sup>, whereas the functionalized electrode material showed 87% capacity retention (Figure 2a).<sup>[34]</sup> The improved capacity retention was attributed to the improved wettability of the electrode and the limitation of the dissolution of LiPSs by introducing the -SH into the cathode.

As one of the most popular carbon hosts, the hollow porous carbons have a macro-pore structure and a large internal cavity volume, which can increase the loading of active material, withstand the volume changes of the cathode during discharge and charge and shorten the transport distance of lithium ions.<sup>[35–37]</sup> Consequently, hollow carbon materials used as sulfur hosts have been widely investigated. Early research on hollow carbon materials as sulfur hosts prone to employ pure carbon materials to trap active materials. In recent years, the combination of hollow carbon with other elements or components not only improves the conductivity of sulfur cathodes, but also promotes the adsorption of intermediate polysulfides. In 2019, Wang et al.<sup>[38]</sup> used urchin-like silicon oxides as a template to prepare a highly uniform N-doped carbon nanosphere as a sulfur host material, which was composed of the radially and inwardly internal aligned supporting ribs, hollow void, and carbon shell. Such a hollow porous carbon structure enhanced the electronic conductivity and maximized the utilization of sulfur. The as-prepared N-doped hollow carbon nanospheres used as sulfur host exhibited a S content of 75% with a capacity of 747

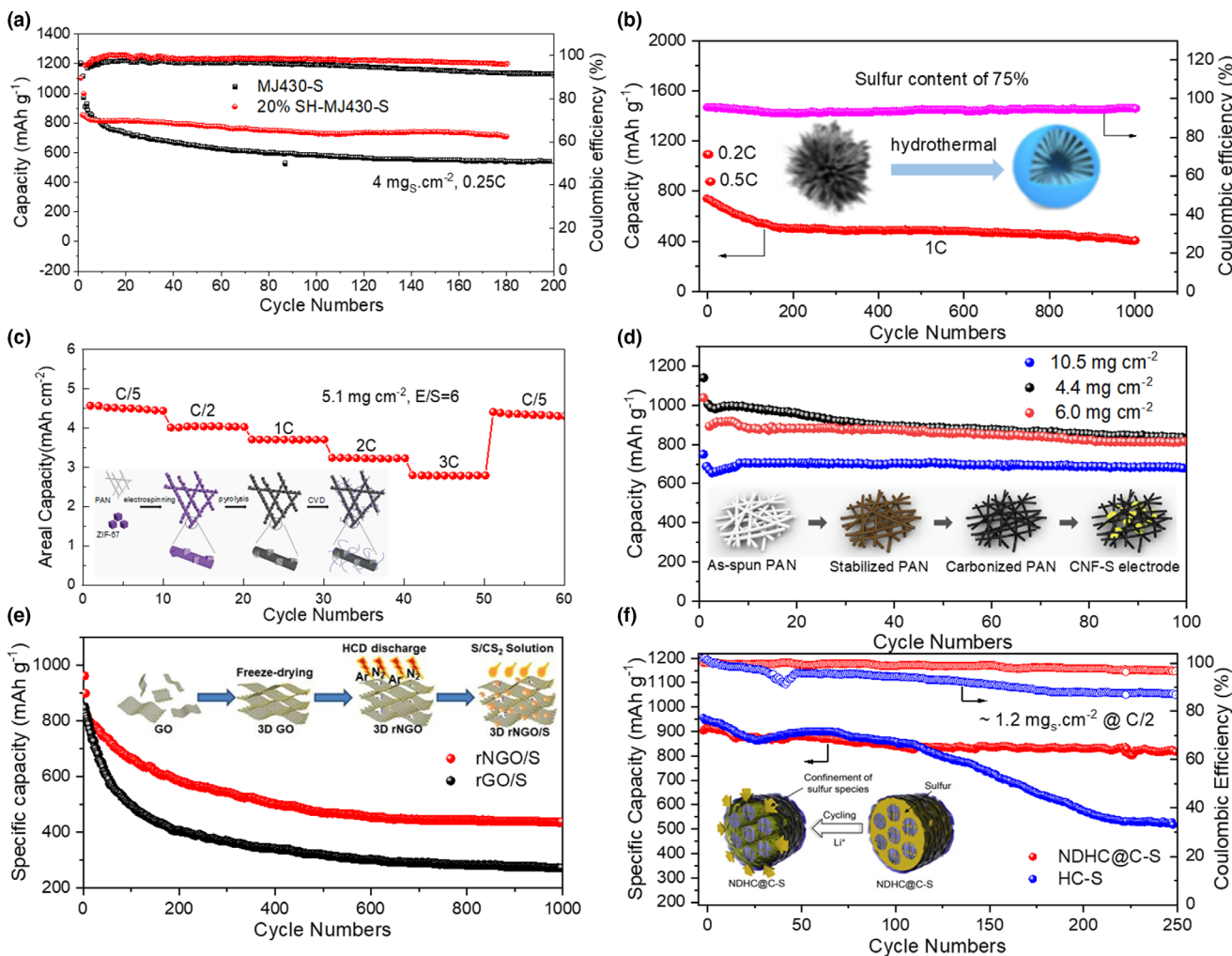


**Figure 2.** Carbon-based materials used as sulfur cathode hosts: a) The thiol surface modifiers enable superior cycle performance of the mesoporous carbon/sulfur composite electrodes. Reproduced with permission.<sup>[34]</sup> Copyright 2019, Royal Society of Chemistry. b) The novel N-doped carbon nanosphere as the sulfur host material enhances the rate capabilities of the Ti-NHCNS<sub>8</sub>/S-75% cathode. Reproduced with permission.<sup>[38]</sup> Copyright 2019, John Wiley and Sons Ltd. c) The rate capability of S@CPZC electrode under sulfur loading of 5.1 mg cm<sup>-2</sup> and E/S ratio of 6 for lithium–sulfur batteries. Reproduced with permission.<sup>[43]</sup> Copyright 2018, Royal Society of Chemistry. d) A CNF-S electrode toward high sulfur loading lithium–sulfur batteries. Reproduced with permission.<sup>[44]</sup> Copyright 2018, American Chemical Society. e) A rNGO/S electrode for lithium–sulfur batteries. Reproduced with permission.<sup>[47]</sup> Copyright 2019, Wiley-VCH Verlag. f) NDHC@C applied as a host for sulfur in lithium–sulfur cathodes. Reproduced with permission.<sup>[29]</sup> Copyright 2020, Elsevier Ltd.

mAh g<sup>-1</sup> at 1 C and achieved high cycle stability over 1000 cycles with a capacity degradation rate of 0.044% per cycle (Figure 2b).<sup>[38]</sup>

Carbon nanotubes (CNTs) have been widely used in Li-S batteries due to their excellent electrical conductivity, high specific surface area, and good mechanical characteristics.<sup>[39]</sup> Recently, Zhang et al.<sup>[40]</sup> designed a novel 3D sulfur host material by integrating the interconnected CNT networks and defective Prussian blue (PB) nano cubes. In this structure, the inter-wave 3D CNT as a conductive skeleton greatly enhanced ion and electron conductivity due to the available efficient lithium-ion and electron channels, while the PB with abundant Lewis acidic sites effectively anchored the soluble polysulfides with Lewis base by Lewis acid–base interaction. Hence, the composite sulfur cathode material demonstrated high capacity, excellent cycle stability, and a long lifespan. However, the energy density of Li-S batteries is closely related to the synergistic relationship between electrode and electrolyte. Low

sulfur loading and a flood of electrolytes will damage the energy density of the battery, which cannot meet the practical applications.<sup>[41,42]</sup> Therefore, it is necessary to design sulfur electrodes rationally to realize high load and low liquid sulfur ratio, to realize a practically viable energy density at the system level. Based on these conditions, Chen et al.<sup>[43]</sup> cleverly developed a stringed “tube on cube” carbonaceous hybrid (denoted as CPZC). The nanohybrid material has a ternary hierarchical architecture, which consists of a fibrous carbon framework, porous carbon cube filler, and the whisker of carbon nanotubes running through the carbon cubes used as novel sulfur for high-performance Li-S batteries. The as-prepared S@CPZC electrode was employed to investigate the rate capability and cycle stability under a high sulfur loading (5.1 mg cm<sup>-2</sup>) and a low E/S ratio (E:S an ratio between the volume of electrolyte and the mass of sulfur) of 6 mL g<sup>-1</sup>. The S@CPZC electrode attained a good area capacity of 2.8

$\text{mAh cm}^{-2}$  at 3 C, and the area capacity returned to  $4.4 \text{ mAh cm}^{-2}$  when the current rate was returned to 0.2 C, demonstrating an excellent electrochemical conversion reaction performance under practical conditions (Figure 2c).<sup>[43]</sup>

Carbon nanofibers (CNFs) are one-dimensional carbon materials with diameters ranging from 10 nm to 500 nm. They hold similar physicochemical properties and morphological characteristics to carbon nanotubes (CNTs) with the ability to improve the conductivity of sulfur species and adsorption capacity of the intermediate soluble polysulfides. Hence, CNFs have been viewed as a promising candidate host material for sulfur composite cathodes. Zheng et al.<sup>[35]</sup> reported hollow CNFs, which were synthesized using anodized aluminum oxide (AAO) membranes as templates, through a polystyrene carbonization process. Combined this hollow CNFs with sulfur as composite materials to effectively trap soluble polysulfides and buffer the volumetric change results in a high capacity of  $730 \text{ mAh g}^{-1}$  over 150 cycles at 0.2 C.<sup>[35]</sup> To realize high sulfur loading and low E/S ratio simultaneously, Lee's group employed an electrospun technique to prepare a novel free-standing CNF material for flexible sulfur cathodes (Figure 2d).<sup>[44]</sup> This design resolved the issue of intermediate polysulfides dissolution and enabled the high mass loading of active materials ( $10.5 \text{ mg cm}^{-2}$ ). Consequently, the produced CNF-S electrode demonstrated a high discharge capacity and excellent cycle stability under a high sulfur loading of  $10.5 \text{ mg cm}^{-2}$ , showing a high reversible capacity of  $752 \text{ mAh g}^{-1}$ , and a capacity retention of 90.4% over 1000 cycles (the average degradation per cycle was only 0.092%) (Figure 2d).<sup>[44]</sup>

Graphene demonstrates excellent electrical conductivity up to  $10^6 \text{ S cm}^{-1}$ , large specific surface areas, and high mechanical properties compared to other carbon materials.<sup>[45,46]</sup> In 2019, Xue and his co-workers designed reduced N-doped graphene (rNGO) with a porous framework by an in-situ hollow cathode discharge plasma (HCD) method.<sup>[47]</sup> As shown in Figure 2e, the freeze-drying approach was used to remove the water from the GO suspension to obtain a 3D GO skeleton. Under flowing argon and nitrogen treatment, the 3D GO framework was reduced and doped by N, resulting in a high-quality 3D rNGO. Finally, the S/CS<sub>2</sub> solution was infiltrated into rNGO to obtain the rNGO/S composite. The porous rNGO framework accelerated ion/electron transfer and inhibited shuttle effects via the chemical binding between nitrogen-doped graphene and polysulfides. As a result, the as-prepared rNGO/S electrode demonstrated a reversible capacity of  $578 \text{ mAh g}^{-1}$  over 1000 cycles at 1 C.<sup>[47]</sup>

To enhance the ability to trap polysulfides, heteroatom doping has been widely employed to modify the carbon hosts to achieve stronger interaction with polysulfides, which can effectively alleviate the shuttle effects and obtain superior electrochemical performance of Li-S batteries.<sup>[48]</sup> Zhang et al.<sup>[49]</sup> designed N-doped carbon nanotubes as sulfur host materials to attain excellent performance for Li-S batteries. Theoretical calculations showed that there were strong Li-N interactions between pyridine nitrogen atoms and various polysulfides. Consequently, the N-doped carbon nanotube–sulfur electrode delivered a high specific capacity of  $937 \text{ mAh g}^{-1}$  at 1 C and the capacity retention of 70% over 200 cycles.<sup>[49]</sup> Recently, Wu et al.<sup>[29]</sup> designed a nitrogen-doped hierarchical porous carbon particle with a microporous carbon shell (NDHC@C) for Li-S batteries. The as-prepared NDHC@C improved the electrical conductivity of sulfur cathodes, and the nitrogen-doped microporous shell offered dual effects of physical confinement and chemical binding with soluble polysulfides. As a result, the NDHC@C-S with a S content of 72% delivered an initial discharge

specific capacity of  $900 \text{ mAh g}^{-1}$  at C/2 and capacity retention of ~90% over 250 cycles (Figure 2f).<sup>[29]</sup>

### 3.2. Polar Inorganic Host

Polar inorganic materials have stronger chemical interactions with polysulfides than nonpolar carbon-based materials, so polar inorganic materials have been employed as sulfur host materials. Polar inorganic materials (metal oxides, metal sulfides, metal nitrides, metal carbides, and so on) employed as sulfur host in Li-S batteries. As a representative example, the Magnéli phase titanium oxide Ti<sub>4</sub>O<sub>7</sub> demonstrating metallic conductivity and intense chemical binding ability toward polysulfides was proposed and employed as a polar host material for high-performance Li-S batteries.<sup>[50]</sup> The Ti<sub>4</sub>O<sub>7</sub> with good conductivity delivered a capacity degradation rate of only 0.06% per cycle within 500 cycles. Very recently, Ding et al.<sup>[51]</sup> elaborately designed a novel catalyst composed of TiO<sub>2-x</sub> nanosheets and reticular CNTs for achieving high performance of Li-S batteries. Through oxygen defect and heterojunction design of titanium oxide, the electronic band structure of titanium oxide can be tuned, which resulted in improved conductivity, strengthened the chemical interaction with LiPSs, and accelerated redox kinetics among LiPSs (Figure 3a). As a result, the as-prepared CNT@TiO<sub>2-x</sub>S electrodes obtained an ultra-high initial specific capacity of  $1204 \text{ mAh g}^{-1}$  at 0.2 C and a capacity of  $867 \text{ mAh g}^{-1}$  over 150 cycles. What's more, the composite cathode showed a capacity of  $700 \text{ mAh g}^{-1}$  over 300 cycles at 1 C, where the capacity retention rate was as high as 87.5% (Figure 3a).<sup>[51]</sup> In addition, some other polar metal oxides have been employed as sulfur host for Li-S batteries, such as Fe<sub>3</sub>O<sub>4</sub>,<sup>[52]</sup> MnO<sub>2</sub>,<sup>[53]</sup> Al<sub>2</sub>O<sub>3</sub>,<sup>[54]</sup> SiO<sub>2</sub>,<sup>[55]</sup> NiFe<sub>2</sub>O<sub>4</sub>,<sup>[56]</sup> and ZnO.<sup>[57]</sup> However, most polar metal oxides used as sulfur host materials must be combined with conductive carbon/polymer materials to improve the conductivity due to the nature of insulation. Wu et al.<sup>[58]</sup> designed a novel Li<sub>2</sub>S cathode with conformal coatings of layered LiTiO<sub>2</sub> for Li and Li-ion batteries. The layered LiTiO<sub>2</sub> shell with excellent electronic and ionic conductivities showed a strong chemical binding with Li<sub>2</sub>S and intermediate polysulfides and accelerated the conversion of long-chain polysulfides to short polysulfides. As a consequence, the as-prepared Li<sub>2</sub>S-LiTiO<sub>2</sub> and Li<sub>2</sub>S@LiTiO<sub>2</sub> electrodes delivered an outstanding rate performance and excellent long-term cycle stability (Figure 3b).<sup>[58]</sup>

Metal sulfides, another class of common polar inorganics, have been developed as sulfur host materials to trap the sulfur species in Li-S batteries. Compared with metal oxides, metal sulfides generally exhibit higher conductivity and some metal sulfides even possess metallic or half-metallic phases. CoS<sub>2</sub> was initially reported in sulfur cathodes for Li-S batteries by Zhang's group in 2015.<sup>[59]</sup> They found that the polar half-metallic CoS<sub>2</sub> electrocatalyst possessed a relatively high conductivity up to  $6.7 \times 10^3 \text{ S cm}^{-1}$  at 300 K, and CoS<sub>2</sub> showed a strong chemical affinity for anchoring the polar LiPSs and accelerating the redox kinetics of sulfur species. The as-prepared graphene/CoS<sub>2</sub> composite as cathode delivered an ultra-high specific capacity of  $1368 \text{ mAh g}^{-1}$  for the initial discharge progress at 0.5 C. Even at a high rate of 2 C, it still exhibited a high capacity of  $1003 \text{ mAh g}^{-1}$  in the first cycle and an average capacity decay rate of 0.034% per cycle. In addition, Cui et al.<sup>[60]</sup> studied the application of TiS<sub>2</sub> in Li-S batteries due to its high conductivity and strong chemical binding with Li<sub>2</sub>S/Li<sub>2</sub>S<sub>n</sub>. The produced core-shell structure of Li<sub>2</sub>S@TiS<sub>2</sub> synthesized by an in-situ reaction was

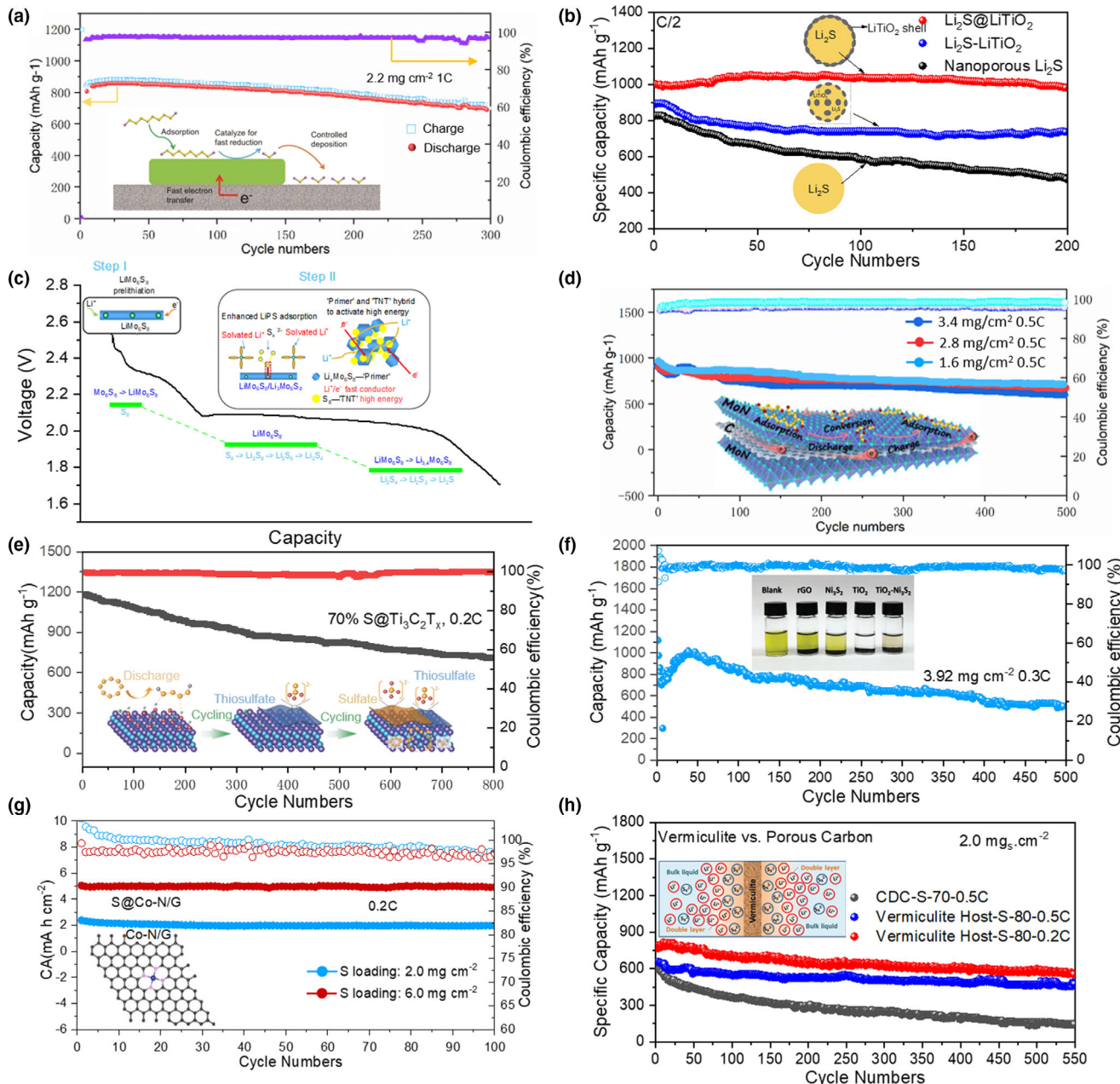


**Figure 3.** Inorganic materials for lithium–sulfur batteries: a) Schematic illustration of CNT@TiO<sub>2-x</sub> regulation of LiPS redox. Reproduced with permission.<sup>[51]</sup> Copyright 2019, Wiley-VCH Verlag. b) Layered LiTiO<sub>2</sub> for the protection of Li<sub>2</sub>S cathodes against dissolution. Reproduced with permission.<sup>[58]</sup> Copyright 2018, Royal Society of Chemistry. c) The roles of the Chevrel-phase Mo<sub>6</sub>S<sub>8</sub> in the hybrid Mo<sub>6</sub>S<sub>8</sub>/S<sub>8</sub> cathode. Reproduced with permission.<sup>[61]</sup> Copyright 2019, Springer Nature. d) The MoN-C-MoN trilayer architecture enabled high-performance lithium–sulfur. Reproduced with permission.<sup>[68]</sup> Copyright 2020, John Wiley and Sons Ltd. e) Ti<sub>3</sub>C<sub>2</sub>T<sub>x</sub> entrapping the polysulfides by forming a sulfate complex protective barrier. Reproduced with permission.<sup>[75]</sup> Copyright 2018, Wiley-VCH Verlag. f) Cycle life of TiO<sub>2</sub>-Ni<sub>3</sub>S<sub>2</sub>/rGO electrode with 3.92 mg cm<sup>-2</sup> sulfur loading. Reproduced with permission.<sup>[76]</sup> Copyright 2020, Wiley-Blackwell. g) cobalt in nitrogen-doped graphene (Co-N/G) as a single-atom catalyst toward high-performance lithium–sulfur batteries. Reproduced with permission.<sup>[79]</sup> Copyright 2019, Wiley-Blackwell. h) The natural Vermiculite is used as a sulfur host in lithium–sulfur batteries. Reproduced with permission.<sup>[81]</sup> Copyright 2019, Wiley-VCH Verlag.

employed as a cathode, demonstrating a high capacity of 503 mAh g<sup>-1</sup> at a high current rate (4 C).

Very recently, Li and his co-workers designed an intercalation–conversion hybrid cathode material by integrating intercalation-type Mo<sub>6</sub>S<sub>8</sub> with electrochemical activity and conversion-type sulfur to achieve

excellent cycle stability and high areal capacity under an extreme condition (about 10% carbon content, E/S = 1.2 μL mg<sup>-1</sup>, high loading >10 mg cm<sup>-2</sup>, low cathode porosity ~ 55 vol %).<sup>[61]</sup> According to the experimental analysis, they found that Mo<sub>6</sub>S<sub>8</sub> offered the ability to contribute its capacity in the ether electrolyte, and its voltage window was

the same as that of S<sub>8</sub>. As shown in Figure 3c, Mo<sub>6</sub>S<sub>8</sub> underwent a three-step transformation during the discharge process. Firstly, Mo<sub>6</sub>S<sub>8</sub> was converted to LiMo<sub>6</sub>S<sub>8</sub> after the pre-lithiation step ( $>2.4\text{ V}$ ). After that, the Li<sub>x</sub>Mo<sub>6</sub>S<sub>8</sub> greatly enhanced the adsorption of long-chain polysulfides and provided a fast channel for lithium-ion due to the intercalation reaction in Li<sub>x</sub>Mo<sub>6</sub>S<sub>8</sub>. Besides, many other metal sulfides have been developed as sulfur host materials, such as MoS<sub>2</sub>,<sup>[62]</sup> NiS<sub>2</sub>,<sup>[63]</sup> Co<sub>3</sub>S<sub>8</sub>,<sup>[64]</sup> and TiS<sub>2</sub>.<sup>[65]</sup> However, the conductivity of metal sulfide is still not enough as sulfur host. To enhance the utilization of active species and reduce the internal impedance, carbon-based materials are still needed to be introduced into cathode materials.

Similar to metal oxides and metal sulfides, polar metal nitrides have inherently excellent conductivity and decent structure stability, resulting in high utilization of active materials and fast redox kinetics during cycles. In 2016, Goodenough et al.<sup>[66]</sup> designed a novel mesoporous TiN, which have high specific surface area, good electrical conductivity, stable porous skeleton, and strong anchoring characteristic, by a solid–solid phase separation method with zinc titanate as an origin material. The mesoporous TiN combined with sulfur as the composite electrode materials displayed a high specific capacity and excellent cycle stability. In the following researches, Mai and co-workers successfully designed a 3D nitrogen-doped graphene/titanium nitride nanowires composite as a free-standing architecture electrode for Li-S batteries, which was synthesized by a facile and effective method.<sup>[67]</sup> Combining the efficient pathways for charge transfer and the strong chemical binding with the polysulfides, the as-prepared electrode with a high active mass loading of 9.6 mg cm<sup>-2</sup> demonstrated an ultra-high areal capacity of 12.0 mAh cm<sup>-2</sup> 4.<sup>[67]</sup> Molybdenum nitrides (MoN) have a decent electrical conductivity ( $4.55 \times 10^6 \text{ S m}^{-1}$ ) and accelerated the redox kinetics of sulfur species. Li et al.<sup>[68]</sup> designed a sandwich structure of MoN-C-MoN as a sulfur cathode host with the synergism of adsorption and catalysis on the continuous catalysis–conduction interface. In this structure, the two outer layers of MoN enabled the strong chemical affinity for polysulfides and their products (Li<sub>2</sub>S<sub>2</sub>/Li<sub>2</sub>S), while the buried C interlayer provided a high-flux charge transfer pathway to enhance the conductivity of the trilayer structure (Figure 3d). Hence, the MoN-C@S electrode exhibited superior cycle stability and long-span cycle life. The discharge capacities still reached up to 604 mAh g<sup>-1</sup> at the high sulfur loading of 3.4 mg cm<sup>-2</sup> over 500 cycles (Figure 3d).<sup>[68]</sup>

Transition metal carbides, carbonitrides, and nitrides (MXenes) are prospective candidates, which have unique 2D construction, excellent conductivity, and abundant surface functionality.<sup>[69]</sup> Their classic configuration is M<sub>n+1</sub>X<sub>n</sub>T<sub>x</sub> (n = 1–3), where M denotes transition metals, X is carbon and/or nitrogen, and T<sub>x</sub> refers to functional groups on the surface, such as hydroxyl, oxygen, or fluorine. Various types of MXene have been synthesized since they were first reported by Gogotsi's group in 2011.<sup>[70]</sup> A large family of MXenes materials including Ti<sub>3</sub>C<sub>x</sub>T<sub>x</sub>,<sup>[70]</sup> Ti<sub>2</sub>CT<sub>x</sub>,<sup>[71]</sup> Mo<sub>2</sub>TiC<sub>2</sub>T<sub>x</sub>,<sup>[72]</sup> and Nb<sub>4</sub>C<sub>3</sub>T<sub>x</sub>,<sup>[73]</sup> have been successfully synthesized for the application in the fields of energy storage. The application of MXene in sulfur host materials for Li-S batteries was initially investigated by Nazar et al.<sup>[74]</sup> They proposed Ti<sub>2</sub>C as a sulfur host. The polar Ti<sub>2</sub>C provided excellent metallic conductivity and strong adsorption to LiPSs, causing a stable capacity up to 723 mAh g<sup>-1</sup> at C/2 over 650 cycles for the Ti<sub>2</sub>C/S electrode. Considering the abundant functional groups on the surface of MXenes, the studies of the interaction between MXenes and polysulfides are extremely significant for designing better sulfur hosts. In 2018, Tang et al.<sup>[75]</sup> elaborately dispersed the sulfur nanoparticles uniformly into polar two-dimensional

Ti<sub>3</sub>C<sub>2</sub>T<sub>x</sub> nanosheets to obtain viscous aqueous ink. After that, a binder-free and flexible electrode was formed by vacuum filtration. The as-prepared binder-free and flexible S@Ti<sub>3</sub>C<sub>2</sub>T<sub>x</sub> electrode demonstrated excellent electrical conductivity and robust structure. It was found that the soluble polysulfides were anchored on the polar Ti<sub>3</sub>C<sub>2</sub>T<sub>x</sub> surface and then were in -situ converted into a thick sulfate complex layer as a protective barrier (Figure 3e). The thick protective barrier significantly alleviated the shuttling of polysulfides during cycling and further resulted in a higher sulfur utilization. Consequently, the free-standing S@Ti<sub>3</sub>C<sub>2</sub>T<sub>x</sub> electrode with 70 wt. % amounts of sulfur exhibited excellent electrochemical performance, including an initial ultra-high capacity of 1184 mAh g<sup>-1</sup> and stability of 724 mAh g<sup>-1</sup> over 200 cycles, in which the capacity decay rate was as low as 0.048%.<sup>[75]</sup>

To combine the advantages of all kinds of metal compounds, a new heterostructure model can be designed to accelerate the redox reaction among polysulfides and simultaneously enhance the chemical adsorption of polysulfides. In this way, the synergistic effect of one material with strong adsorption and another material with fast electron transfer can ensure smooth trapping–diffusion–conversion of polysulfides and improve the utilization of active species. Considering the desirable benefits from heterostructures, Yang's group proposed heterostructure (TiO<sub>2</sub>–Ni<sub>3</sub>S<sub>2</sub>) as a bidirectional catalyst, which can accelerate both the reduction of long-chain polysulfides and the oxidation of short-chain polysulfides.<sup>[76]</sup> According to their results, TiO<sub>2</sub> and Ni<sub>3</sub>S<sub>2</sub> loaded on the reduced graphene oxide (rGO) played two roles in the adsorption of polysulfide and acceleration of electron transfer, respectively, which could synergistically promote the transformation of polysulfides. In the reduction process, TiO<sub>2</sub> provided a strong capturing effect on soluble polysulfides, and Ni<sub>3</sub>S<sub>2</sub> catalyzed the reduction process and regulated the deposition behavior of the reduced product Li<sub>2</sub>S. Therefore, the assembled battery with high sulfur loadings of 3.92 mg cm<sup>-2</sup> delivered a stable discharge capacity of 504 mAh g<sup>-1</sup> at 0.3 C over 500 cycles and a capacity retention of 63% (Figure 3f).<sup>[76]</sup>

Although employed catalysts in sulfur host materials can accelerate the redox conversion of polysulfides, excessive use of catalysts will decrease sulfur loading while reducing the practical energy densities. In addition, compared with sulfur, metal-based catalysts are relatively expensive, which would cause an increase in the cost of Li-S batteries. Considering problems as mentioned above, single-atom catalysts (SACs) have been regarded as favorable catalysis due to the maximized atom utilization.<sup>[77]</sup> In 2018, Yang and his co-workers initially studied the application of SACs on lithium–sulfur batteries to promote the reversible transformation of S and LiPSs.<sup>[78]</sup> The authors designed a porous carbon material as sulfur host, which have abundant single-atom Fe active sites on its surface. The as-prepared sulfur cathode with Fe SACs delivered a stable discharge capacity of 557.4 mAh g<sup>-1</sup> at 0.5 C over 300 cycles and a capacity decay rate as low as 0.2% per cycle within 300 cycles. Experimental studies have demonstrated that the single-atomic iron active sites as electrocatalytic active substances promoted the soluble polysulfides redox kinetics. This work opened a completely new way for the catalytic conversion of polysulfides.<sup>[78]</sup> Except for Fe SACs, Co SACs were also considered as promising SACs for promoting the polysulfides conversion. Ji et al.<sup>[79]</sup> firstly reported nitrogen-doped graphene embedded with monodispersed cobalt atoms can be employed as sulfur host material for Li-S batteries, accelerating the conversion of polysulfides. By model analysis and atomic-scale characterization, the authors concluded that Co atoms were dispersed in the nitrogen-doped graphene lattice and coordinated to four nitrogen ligands to form Co-N-C coordination centers. Therefore, the S@Co-N/

G cathode with an ultra-high S mass ratio of 90% exhibited an ultra-high specific capacity of  $1210 \text{ mAh g}^{-1}$ . Furthermore, the S@Co-N/G electrode exhibited an areal capacity of  $5.1 \text{ mAh cm}^{-2}$  and a capacity attenuation rate as low as 0.029% per cycle over 100 cycles at 0.2 C under the sulfur loading of  $6 \text{ mg cm}^{-2}$  (Figure 3g).<sup>[79]</sup>

In addition to complex metal compound designs, some naturally abundant minerals were employed as functional sulfur hosts or additives for Li-S batteries. For example, Yuan et al.<sup>[80]</sup> constructed a novel composite material, including natural sepiolite (Sep) powders, CNTs and conductive polymer (PANI). The as-prepared Sep/CNT/S@PANI electrode displayed an initial ultra-high capacity of  $\sim 1100 \text{ mAh g}^{-1}$  at 2 C and a capacity of  $650 \text{ mAh g}^{-1}$  after 300 cycles. In recent years, Wu et al.<sup>[81]</sup> reported a promising host material that is the naturally abundant and inexpensive natural clay mineral, which was applied in Li-S batteries. The natural mineral viz. vermiculite with layered structure effectively reduced polysulfides dissolution and the shuttle effects because of the presence of surface cations on the vermiculite surface, which exhibited strong interaction with polysulfides anions. As a result, compared with the carbon-S electrodes, the vermiculite-S electrodes exhibited outstanding rate capabilities, and desirable long-term cycle stabilities (Figure 3h).<sup>[81]</sup>

### 3.3. Organosulfur Compounds

Organosulfur compounds have been viewed as attractive candidates due to their self-protection of sulfur species. In addition, most of them are inexpensive, easy to fabricate, and environmentally friendly. According to previous studies, their properties and electrochemical behavior can be regulated by tuning functional groups.<sup>[82]</sup> In 1988, organosulfide compounds were first used as cathode materials by Visco and DeJonghe.<sup>[83]</sup> Then, organosulfides have been widely studied and various progresses have been achieved, which are generally divided into two categories: organosulfide polymers and organosulfide molecules.

The organosulfide polymer is a promising composite material encapsulated sulfur material, working as sulfur cathodes. Functional or conductive polymer materials (e.g., polypyrrole, polyaniline, poly(3,4-(ethylenedioxy)thiophene) (PEDOT)) were widely employed to synthesize a variety of organosulfide polymer composite materials with regulated morphologies. For example, several conducting polymers as a conductive substrate and/or as a protective layer to anchor intermediate polysulfides were successfully constructed. Park and his Co-workers reported a 3D interconnected organosulfur polymer with controllable morphology, which was synthesized by a soft template of porous tri thiocyanic acid (TTCA) crystals.<sup>[84]</sup> The as-prepared polymer employed as active electrode material exhibited excellent rate capability because the amine groups of TTCA within the polymer framework facilitated Li ions transport. Consequently, the produced organosulfur polymer enabled a specific capacity of  $850 \text{ mAh g}^{-1}$  at 450th cycle with over 83% capacity retention (Figure 4a). In addition to artificially synthesized polymers, natural harmless polymers used as cathode materials are more in line with the development of green energy. Taking that into account, Wu et al.<sup>[85]</sup> innovatively designed a sulfur-limonene polysulfide (SLP) as sulfur cathode material for Li-S batteries. Sulfur-limonene polysulfide can be synthesized through a simple one-pot reaction on a large scale using abundant, low-cost, and environmentally friendly raw materials sublimed sulfur powder and d-limonene. After the first discharge, the long sulfur chains in the as-produced SLP were nonreferring transformed to lithium sulfides, and  $S_8$  and

sulfur-limonene disulfide were generated in the subsequent charging process (Figure 4b). However, this irreversible phase change during the first cycle resulted in an embedded structure in situ that was self-protection, protecting the active sulfur species from polysulfide shuttle effects. The free-standing electrode with sulfur loading of  $3.0 \text{ mg cm}^{-2}$  received a high specific capacity of  $956 \text{ mAh g}^{-1}$  at 0.5 C and a ultra-high Coulombic efficiency about 99.9%.<sup>[85]</sup>

All the organosulfide polymers mentioned above have a solid–liquid–solid (SLS) phase transition path. In addition, the conversion path of polymer sulfur can be solid–solid (SS) transformation mechanism. During the charging and discharging process, these polymer materials with SS conversion will be changed into  $\text{Li}_2\text{S}_2/\text{Li}_2\text{S}$  and some other organic compounds. Thus, soluble polysulfides will not be generated during the conversion process. In 2002, Wang and his group initially proposed that the heating mixture of acrylonitrile and sulfur synthesized sulfurized polyacrylonitrile (SPAN), which can be employed as a cathode material.<sup>[86]</sup> Ming and his co-workers innovatively proposed a mechanism to explain the electrochemical behavior of SPAN in Li-S batteries.<sup>[87]</sup> They found that a thiy radical was generated after the sulfur–sulfur bond broke in initial cycle, then formed a conjugated structure due to electron delocalization of the sulfur radicals on pyridine backbone (Figure 4c). The conjugative structure can react with lithium ions through a transfer process of lithium coupled electron and form an ion-coordination bond reversibly. This unique reaction mechanism enabled SPAN as a cathode material to obtain excellent cyclic stability and excellent rate capability.<sup>[87]</sup> However, SPAN-based cathodes are limited by the less than 50 wt.% sulfur content, which is hard to meet the high energy characteristics of practical Li-S batteries. As a feature, SPAN-based electrodes can be normally cycled in carbonate electrolyte systems. However, based on some established kinds of literature, ether electrolytes are more compatible with lithium metal anode than carbonate electrolytes. To solve the problems mentioned above, selenium (Se) is incorporated into the sulfur chain in SPAN, which not only makes SPAN compatible with ether electrolytes but also promotes the transformation of soluble intermediates.<sup>[88]</sup> According to experimental analysis, the catalytic amount of Se-doping increases the lithium-ion diffusion coefficient in the electrode, resulting in the fast redox conversion between long-chain and short-chain polysulfides, and alleviating the dissolution of polysulfide intermediates in ether electrolytes. Therefore, the  $\text{Se}_{0.06}\text{SPAN}$  as cathode delivered an ultra-high capacity of  $1156 \text{ mAh g}^{-1}$  in the second cycle and a capacity decay rate of 0.029% per cycle (Figure 4d). In addition, the whole mass of  $\text{Se}_{0.06}\text{SPAN}$  electrode still exhibited a capacity of  $546 \text{ mAh g}^{-1}$  at the second cycle, and the capacity stayed at  $416 \text{ mAh g}^{-1}$  after 800 cycles (Figure 4d).<sup>[88]</sup>

Compared to organosulfide polymers, organosulfide molecules contain sulfur chains with a lower molecular weight, which have been widely studied. In 2018, Fu and his co-workers investigated the incorporation of sulfur into phenyl diselenide (PDSe, PhSeSePh) in different proportions (1:1 and 1:2 molar ratios).<sup>[89]</sup> The as-produced phenyl selenosulfides (PDSe-S, PDSe-S<sub>2</sub>) were employed as cathodes for rechargeable lithium–sulfur batteries. As shown in Figure 4e, these hybrid materials exhibited unique electrochemical behavior with three reversible discharge platforms, which involved multiple Se–S and S–S bond breakage and their formation. Consequently, PDSe-S and PDSe-S<sub>2</sub> showed higher specific capacities and coulombic efficiencies than PDSe. In addition, 4,4'-dipyridyl disulfide (4,4'-DpyDS), 2,2'-dipyridyl disulfide (2,2'-DpyDS), and 2,2'-dipyridyl disulfide-N,N'-dioxide (DpyDSDO) were studied by Fu et al.<sup>[90]</sup> Compared with DPD, 2,2'-DpyDS and 4,4'-DpyDS showed a higher discharge platform (2.45V)

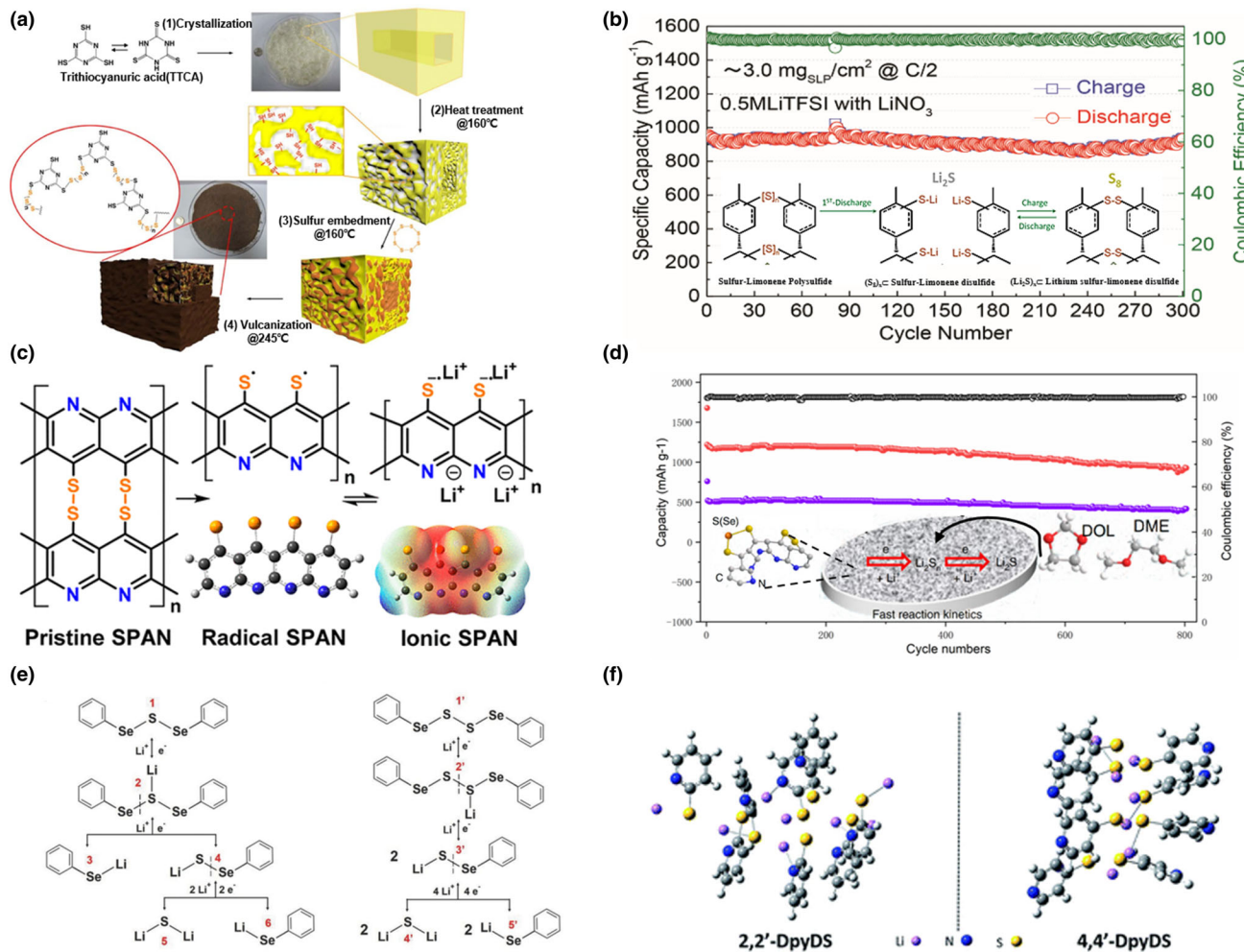


**Figure 4.** Organic materials for lithium–sulfur batteries: a) Synthesis of 3D interconnected sulfur-rich polymer. Reproduced with permission.<sup>[84]</sup> Copyright 2015, Springer Nature. b) a sulfur–limonene-based cathode for lithium–sulfur batteries. Reproduced with permission.<sup>[85]</sup> Copyright 2018, Wiley-Blackwell. c) Lithiation process of SPAN. Reproduced with permission.<sup>[87]</sup> Copyright 2018, American Chemical Society. d) Se-doped SPAN is used in ether-based electrolytes. Reproduced with permission.<sup>[88]</sup> Copyright 2019, Springer Nature. e) Reversible redox transformation of PDSe-S and PDSe-S2. Reproduced with permission.<sup>[89]</sup> Copyright 2018, Wiley-VCH Verlag. f) Cluster structures of the discharge products of 2,2'-DpyDS and 4,4'-DpyDS. Reproduced with permission.<sup>[90]</sup> Copyright 2019, Royal Society of Chemistry.

than that of DPDS (2.2V), indicating the pyridine functional group in organodisulfides can increase the discharge voltage platform. However, DpyDSO showed the highest discharge voltage platform of 2.8V. The electrochemical analysis showed that 2,2'-DpyDS and 4,4'-DpyDS had a remarkable difference in electrochemical performance as capacity retention and cycling stability. This significant difference was attributed to the different solubility of discharge products in electrolytes. As the discharge product of 2,2'-DpyDS, lithium pyridine-2-thiolate can form dense cluster structure through N···Li···S bridges, while lithium pyridine-4-thiolate cannot.<sup>[90]</sup>

### 3.4. Flexible Sulfur Cathode

Compared to conventional cathodes produced by slurry casting technology, the free-standing electrode can avoid the use of binder and current collector, while increasing the active sulfur content in cathodes.

A cathode with high areal sulfur loading can be easily achieved by stacking free-standing or flexible sheets. In addition, the high mechanical strength skeleton can withstand the long-term operation under folding and bending, which is important to future flexible devices.

CNTs have been widely studied due to the unique structure and features, since it was first proposed by Iijima in 1991.<sup>[91]</sup> The easily controllable porous structure in CNTs-based materials and their interior can provide sufficient space and 3D interconnected bridges for Li<sup>+</sup>/e<sup>-</sup> transports. The decent mechanical properties can protect the material from the adverse effects of volumetric and structural changes. Very recently, Lee et al.<sup>[92]</sup> elaborately designed a novel kind of nanomat Li-S batteries with super high energy density and appropriate mechanical flexibility. The unique cathodes composed of fibrous mixtures of sulfur-deposited multi-walled CNTs and single-walled CNTs were combined with bi-layered separators to form all-fibrous cathode-separator assemblies (Figure 5a). The as-prepared nano Li-S batteries including the assemblies of cathode and separator and conductive nonwoven-

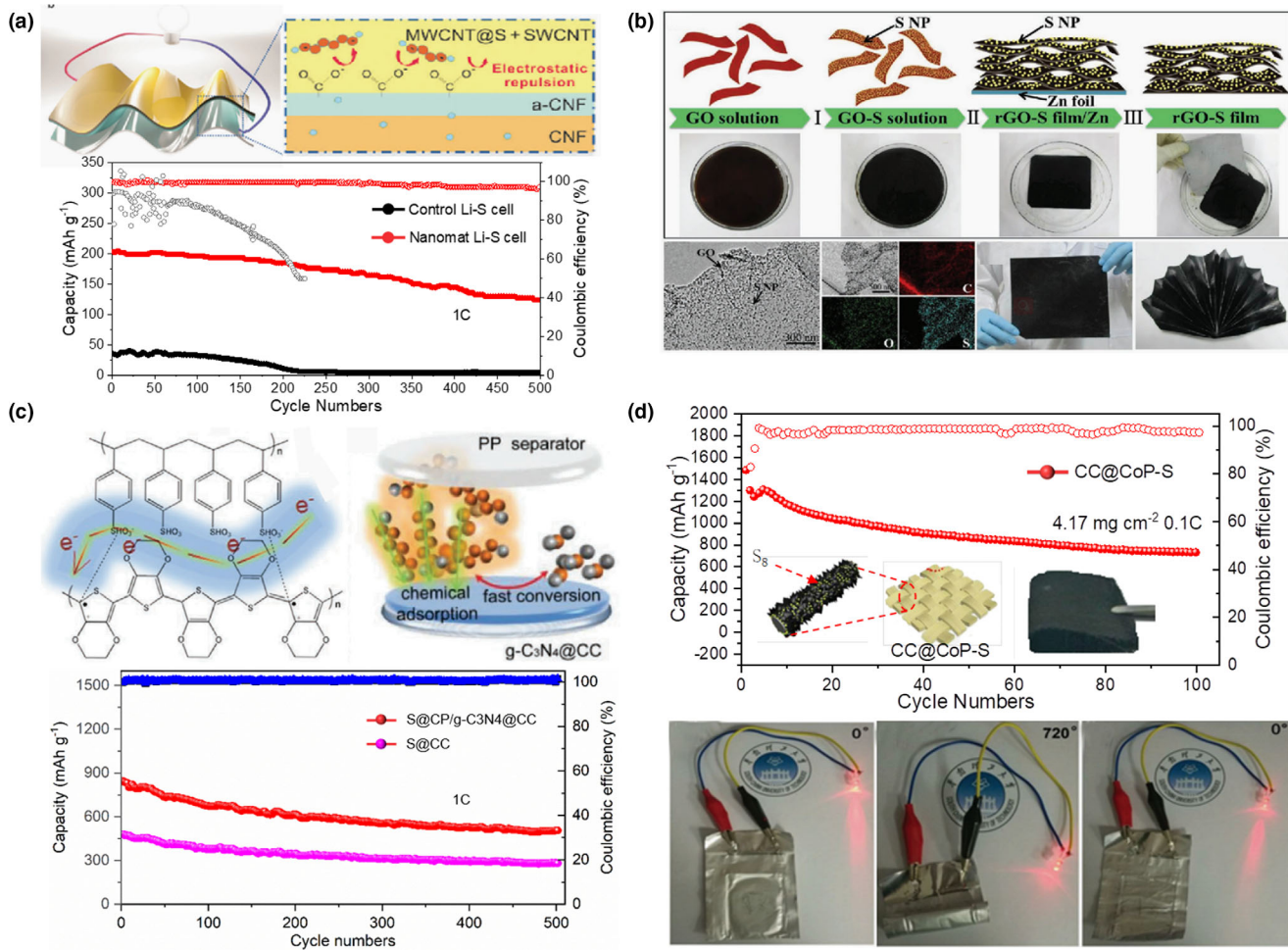


**Figure 5.** Flexible materials for lithium–sulfur batteries: a) Cycling performance of the control and nanomat Li–S cells at 1C. Reproduced with permission.<sup>[92]</sup> Copyright 2019, Royal Society of Chemistry. b) Self-assembled graphene-based flexible sulfur cathodes. Reproduced with permission.<sup>[94]</sup> Copyright 2016, Wiley-Blackwell. c) S@CP/g-C<sub>3</sub>N<sub>4</sub>@CC cathode for high-performance lithium–sulfur batteries. Reproduced with permission.<sup>[95]</sup> Copyright 2020, Wiley-VCH Verlag. d) CC@CoP/C-S cathode for flexible lithium–sulfur batteries. Reproduced with permission.<sup>[96]</sup> Copyright 2019, Wiley-Blackwell.

reinforced Li metal anodes enhanced the redox kinetics, flexibility, and cycle performance, delivering a high energy density and long lifespan more than 500 cycles with a small decay rate of 0.07%.<sup>[92]</sup> Zhou et al.<sup>[93]</sup> employed graphene foam which demonstrated remarkable electrical conductivity, strong mechanical stability, and enough space to build flexible Li–S batteries. The as-prepared flexible cathode with a sulfur loading of 10.1 mg cm<sup>-2</sup> received a capacity of 448 mAh g<sup>-1</sup> after 1000 cycles, and a capacity decay rate of 0.071% per cycle. Niu et al.<sup>[94]</sup> constructed a flexible sulfur cathode using the reduced graphene oxide (rGO) as a host (Figure 5b). In the specific synthesis of details, sulfur powders with a particle size of 9–22 nm were deposited on the GO sheet by an in situ reaction in Na<sub>2</sub>S<sub>2</sub>O<sub>3</sub> solution. The zinc foil was then immersed in a solution of GO–S to obtain a dense rGO–S film. During the reaction, electrons transfer to the Zn foil and GO, leading to the production of zinc ions and rGO, which bind firmly to the Zn foil. This synthesis method was highly efficient for the preparation of flexible rGO composites. The as-prepared rGO–S thin film with good tensile strength (68 MPa) withstood varying degrees of bending and crimping. Zheng and his co-workers successfully designed a novel flexible sulfur cathode, which was synthesized by integrating sulfur,

carbon nitride (g-C<sub>3</sub>N<sub>4</sub>) film, and flexible carbon cloth covering a conductive polymer (CP).<sup>[95]</sup> The as-prepared S@CP/g-C<sub>3</sub>N<sub>4</sub>@CC cathode showed distinct advantages employed for Li–S batteries. The g-C<sub>3</sub>N<sub>4</sub> surface was covered with abundant active adsorption sites of pyridinic-N, which effectively absorbed polysulfides, retarded the dissolution of polysulfide, and enhanced the polysulfides redox conversion. Therefore, the S@CP/g-C<sub>3</sub>N<sub>4</sub>@CC electrode exhibited a reversible specific capacity of 516.9 mAh g<sup>-1</sup> at 1 C after 500 cycles (Figure 5c). Wang et al.<sup>[96]</sup> designed a flexible sulfur cathode material by integrating elemental sulfur, flexible conductive carbon cloth (CC), and N-doped nanosheets embedded with CoP (CoP/C). The as-prepared CC@CoP/C-S composite cathode demonstrated several advantages such as a desirable electrical conductivity, high sulfur loading, excellent physical and chemical adsorption of polysulfides, and catalytic effects by CoP nanoparticles (enhancing the conversion reaction kinetics among polysulfides), which exhibited a capacity of 1257 mAh g<sup>-1</sup> after 100 cycles at 1.81 mg cm<sup>-2</sup> and obtained 737 mAh g<sup>-1</sup> over 100 cycles even under the sulfur loading of 4.17 mg cm<sup>-2</sup> (Figure 5d). What's more, the author investigated the influence of Li–S pouch cell on light-emitting diode (LED) lighting under different folding levels. The

experiment demonstrated that the Li-S pouch cells can withstand 90°, 180°, and 720° bending without affecting LED lighting (Figure 5d), indicating the cell is not affected by the folding processes.<sup>[96]</sup>

Overall, each of above host materials has its own advantages and disadvantages. Carbon materials have been widely used as sulfur host materials during the early stage of Li-S batteries due to their high electrical conductivity and diversity in nanostructures, but the cycling performance is not satisfactory because the nonpolar carbon can only provide weak physical adsorption for the polar LiPSs. The organic materials have a lot of functional groups and the flexible and elastic nature of polymer can accommodate the volume variation; however, the conductivity and thermal stability of organic materials are not as good as most of the carbon materials. Compared with nonpolar carbon, polar host materials reveal much stronger chemical anchoring of polysulfides, which can mitigate the polysulfide loss and improve sulfur utilization, but their synthesis processes are complicated. Therefore, the characteristics of different materials should be taken into consideration when designing cathodes.

#### 4. Electrolyte

The electrolyte as a bridge between sulfur cathode and lithium anode bears a path for ion transportation, which has a significant effect on the electrochemical behaviors of Li-S batteries for different solubility of polysulfides (LiPSs) in various electrolyte solvents.<sup>[12,97–99]</sup> The studies found that the chemical and electrochemical procedures of the sulfur redox reactions were strongly influenced by the solvation structure of the polysulfide anions.<sup>[100]</sup> Molecular dynamics simulations can be adopted to research the inherent stability of dissolved polysulfide, thus helping to understand or predict the types of related chemicals present in the solvent at low concentrations as well as the dynamic behavior at equilibrium.<sup>[101,102]</sup> In general, the dielectric constant ( $\epsilon$ ) of the solvent is related to the stability of polar or ionic solute species, and the Donor Number (DN) is directly connected with the complexation between the cation and the solvent molecules. In particular, the solvent with higher DN and  $\epsilon$  is more favorable to the formation of bound LiPS, and vice versa.<sup>[103]</sup> As shown in Figure 6, when designing a lithium–sulfur battery electrolyte with a specific function, we should consider the following main factors in order—the  $\epsilon$  and DN of solvent, the sulfur speciation pathway, the concentration and amount of lithium salts and the additives. As a result, the high- $\epsilon$ , high-DN, and low-viscosity electrolytes have the potential to achieve the demanding engineering conditions, such as a high sulfur utilization.<sup>[104]</sup> In order to realize a target energy density of 400–500 Wh kg<sup>-1</sup>, building high-performance Li-S batteries using low electrolyte/sulfur (E/S) ratio and thick sulfur cathodes are necessary; meanwhile, the shuttling of polysulfides and unstable lithium metal anode should be overcome.<sup>[105]</sup>

##### 4.1. Organic Solvent-Based Electrolyte

For sulfur/carbon cathode materials, the low-viscosity ethereal solvents such as 1,2 dioxolane (DOL) and 1,3 dimethoxyethane (DME) are largely employed. However, the poor electrochemical stability and high volatility of the conventional ether-based solvents, especially DME, prevent them from commercial applications. Typically, the commonly used solvents DOL/DME (1:1 by volume) will interact with the dissolved LiPSs through solvation. High concentration of lithium

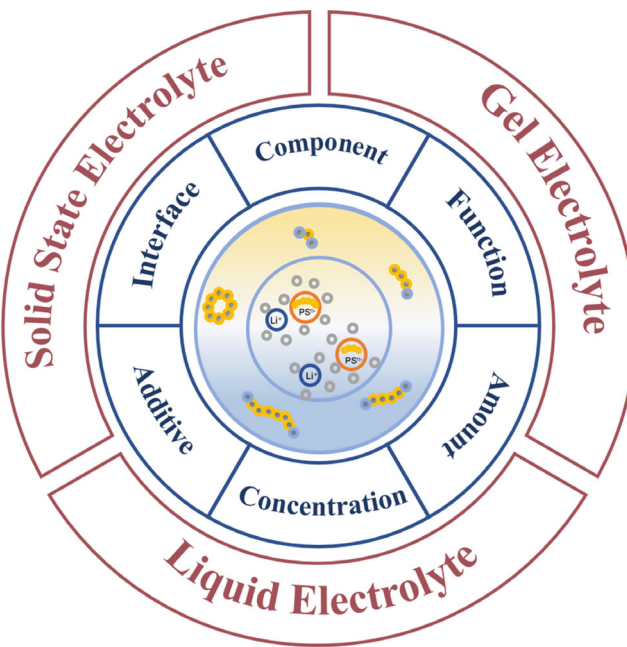


**Figure 6.** The design criteria of electrolytes in Li-S batteries.

polysulfide will quickly reach the saturation mode when using the low E/S ratio, causing the reduction of ionic conductivity and premature precipitation of LiPSs.<sup>[106]</sup>

To remedy this, some breakthroughs have been achieved in ether-based solvents. Fluorinated ether can be used as co-solvent for the low solubility to polysulfide anion in order to change the Li-ion solvation mode and form a stable solid electrolyte interphase (SEI) via a reductive decomposition. Zhang et al. studied the relationship between the pattern of fluorination in a partially fluorinated ethers (PFE) solvent and Coulombic efficiency. As a result, the high fluorine content of functioning PFE solvents can amend the Coulombic efficiency and specific discharge capacity retention in Li-S cells. For example, the 1,1,2,2-tetrafluoroethyl 2,2,3,3-tetrafluoropropyl ether (TTE) working as a co-solvent provided an excellent Coulombic efficiency of 95% after 100 cycles under the E/S of 10 mL g<sup>-1</sup>.<sup>[107]</sup> In addition, because of the reduced polysulfide solubility, a fluorinated ether 1,2-(1,1,2,2-tetrafluoroethoxy)ethane(TFEE)-based electrolyte presented excellent Coulombic efficiencies at a low E/S ratio.<sup>[108]</sup> However, the reduction of the volume of electrolyte in these works always comes with increased polarization and cost.

An increase in salt concentration will lead to increased interactions between cationic and anion/solvent and a decrease in the free solvent molecule content, as well as the location of the lowest unoccupied molecular orbital (LUMO) move from the solvent to the salt, which enables decomposition of the solvent at lower potential than the salt.<sup>[109–111]</sup> However, such electrolytes typically performed low-capacity utilization and reduced practical energy density along with high viscosity, low Li-ion mobility and poor wettability on S cathodes under low E/S ratio and high sulfur loading.<sup>[112,113]</sup> However, it is surprising that Nazar and her colleagues turned the electrolyte network construction into quasi-solid-state sulfur conversion by improving the concentration of electrolyte in a diethylene glycol dimethyl ether system (G2:LiTFSI) under low E/S ratio (5  $\mu$ L mg<sup>-1</sup>).<sup>[114]</sup> As shown in

**Figure 7a**, the pressurized pouch cells in G2: LiTFSI (0.8:1) electrolyte demonstrated a more steady capacity of 720 mAh g<sup>-1</sup> over 100 cycles than those in G2:LiTFSI (7:1) electrolyte, which was attributed to the depletion of the electrolyte.<sup>[114]</sup> The ab initio molecular dynamics

(AIMD) calculations displayed that there was a stronger association between Li<sup>+</sup> and TFSI<sup>-</sup> at low G2: LiTFSI ratios with the maintain of Li-G2 coordination, which generated a reinforced three-dimensional (3D) network. In this atmosphere, each TFSI<sup>-</sup> bonded with multiple

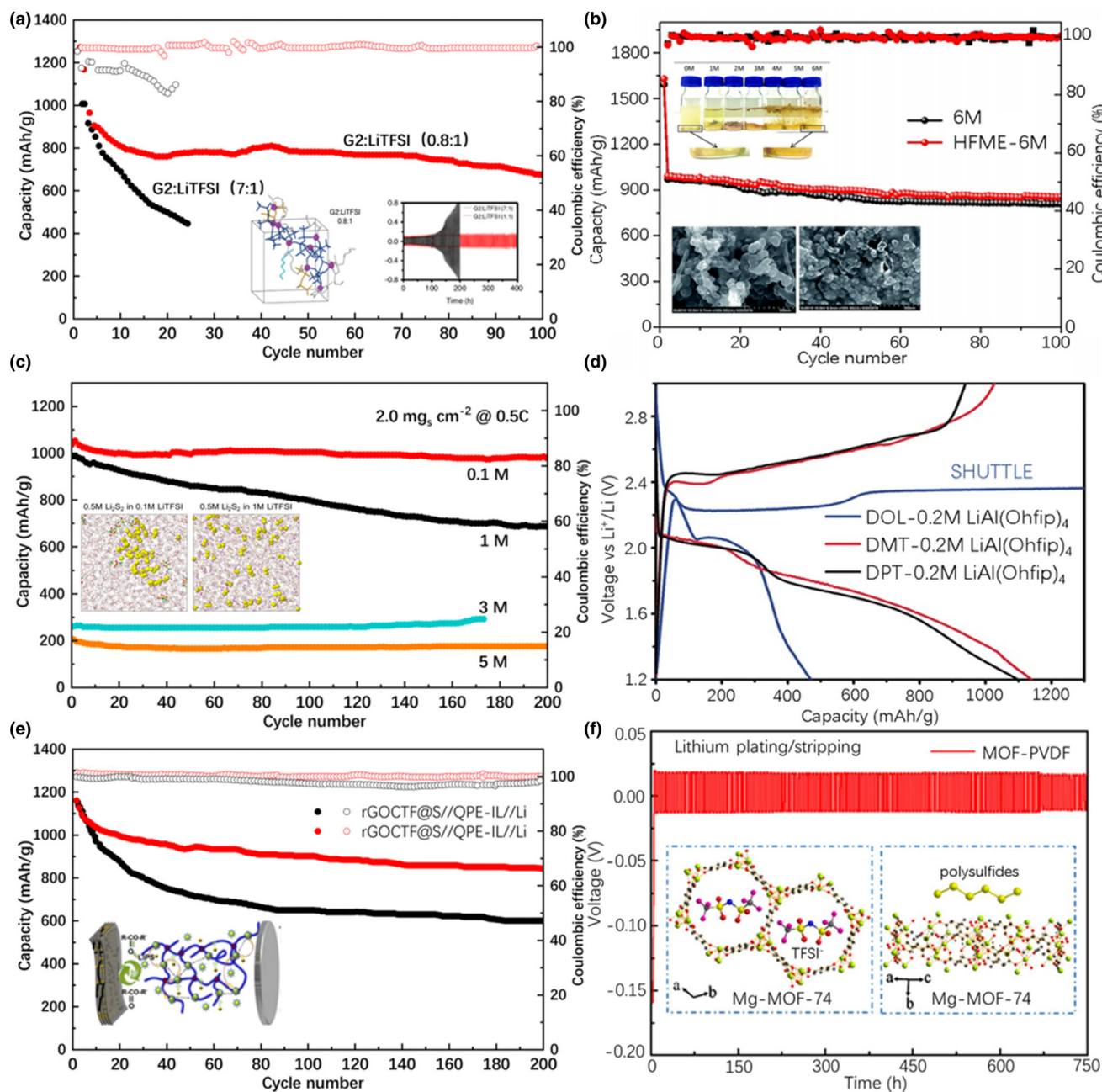


**Figure 7.** The performance improvement strategies for different types of electrolytes in Li-S batteries: a) The cycling performance of different solvent/salt molar ratio in a diethylene glycol dimethyl ether system (G2:LiTFSI) under low E/S ratio of 5  $\mu\text{L mg}^{-1}$  at C/5; Reproduced with permission.<sup>[114]</sup> Copyright 2018, Springer Nature. b) High-performance Li-S batteries based on the high concentration carbonate electrolyte(6 M LiTFSI in EC/DEC); Reproduced with permission.<sup>[121]</sup> Copyright 2019, Royal Society of Chemistry. c) The excellent cycling performance at 0.5 C of the CC-S cathode in a super-diluted (0.1 mol L<sup>-1</sup>) of LiTFSI in DME/DOL with 1 wt. % LiNO<sub>3</sub>) electrolyte; Reproduced with permission.<sup>[115]</sup> Copyright 2020, American Chemical Society. d) Discharge/charge profiles of S@pPAN cathodes in new electrolyte system; Reproduced with permission.<sup>[117]</sup> Copyright 2017, John Wiley and Sons Ltd. e) Cycling performances of the rGOCTF@S//QPE-IL//Li battery; Reproduced with permission.<sup>[127]</sup> Copyright 2019, American Chemical Society. f) Schematic illustration of MOF-PVDF GPE with anions immobilized and Li plating/stripping behavior of Li/Li symmetrical cell; Reproduced with permission.<sup>[129]</sup> Copyright 2019, American Chemical Society.

$\text{Li}^+$ , resulting in a lower fraction of free solvent and leading to low solubility of polysulfide and weak reactivity with Li, which turned the reaction mechanism of sulfur from the conventional dissolution–precipitation to a quasi-solid-state reaction. The electrolyte system not only turned the sulfur speciation pathway, but also suppressed parasitic reaction on the Li anode.<sup>[114]</sup> However, the cells were operated at 55 °C, which still need further optimization in physicochemical properties, including viscosity and ionic conductivity, as well as the cycle performance.

Very recent, a system based on the experimental and theoretical studies demonstrated that a super-diluted (0.1 mol L<sup>-1</sup> of LiTFSI in DME/DOL with 1 wt. % LiNO<sub>3</sub>) electrolyte successfully enabled high-performance Li-S batteries, which is promising for future practical Li-S cells under high sulfur loading and low electrolyte volume.<sup>[115]</sup> According to their results, compared to standard 1 M and concentrated electrolytes, the super-dilute electrolyte presented much better and faster wetting properties, which is beneficial to capacity utilization at the moderate C rates from 0.5 C to 2 C. In addition, super-dilute electrolyte is much more cheap and lighter, which generates benefits for future low-cost, high energy density batteries. Concerning the promising cycle stability in the super-dilute electrolyte, the combination of MD simulations and experiments demonstrated that the super-dilute electrolyte offered extraordinary ability of suppressing the dissolution of short-chain polysulfide and polysulfide shuttling. As shown in Figure 7c, the cell using 0.1 M electrolyte showed an excellent capacity retention of ~95% over 200 cycles at moderate C/2 rate, distributing a discharge capacity of ~970 mAh g<sup>-1</sup> at the 200<sup>th</sup> cycle and forming a sharp contrast with the cells in 1 M and higher concentration electrolytes.<sup>[115]</sup> More studies about dilute electrolytes in Li-S chemistry should be studied in details in future, such as the in situ change of ionic transport at the interface during the discharge.

Recently, some new ether solvents have been well studied. For example, Wang et al.<sup>[116]</sup> reported a concentrated electrolyte of 4 M LiTFSI/ dibutyl ether(DBE), in which the DBE could inhibit the dissolution of lithium polysulfides definitely, with an excellent Coulombic efficiency of ~99.2% in Li/S@pPAN cells. Nazar et al.<sup>[117]</sup> proposed a new electrolyte system consisted of lithium tetrakis (hexafluoroisopropoxide) aluminum (Li[Al-(Ohfp)<sub>4</sub>]) salt, N,N-dimethyl triflimide (DMT) and N,N-dipropyl triflimide(DPT). Since the solvent is hydrophobic and the salt is low ion-pairing, the battery could demonstrate a high reversible capacities (1200–1500 mAh g<sup>-1</sup>) at a wide current density range (C/5–2C) and a high Coulombic efficiency (>99.7%) without the presence of LiNO<sub>3</sub> at 50 °C (Figure 7d).

Owing to the side reaction between carbonate solvents and soluble polysulfides, the carbonate-based electrolyte has long been thought not to be an electrolyte for Li-S batteries.<sup>[118]</sup> However, carbonate solvents were chosen to pair with various sulfur molecules in cathode materials.<sup>[12]</sup> As a result, different carbonate-based electrolytes were investigated to decide the influence of the structure of the solvents on the electrochemical performance of SPAN-based Li-S cells. For example, linear carbonates (DMC; DEC; DPC; and EGBMC) were investigated in combination with FEC as electrolytes in SPAN-based cells, and lower viscosities of the carbonates gave higher specific capacities. The combination of DMC and FEC electrolyte system worked best and 3 M LiTFSI (in FEC and DMC) showed an excellent cycle stability with a specific capacity of 990 mAh g<sup>-1</sup> over 600 cycles at 0.5 C.<sup>[119]</sup> Besides, A high capacity of 1270 mAh g<sup>-1</sup> was achieved in LiTFSI/EMC-FEC (7:3) electrolyte after 1000 cycles at 2 C.<sup>[120]</sup> As another strategy, change of the solvation structure of electrolyte successfully achieved the compatibility

between the standard sulfur cathode and the modified carbonate-based electrolytes.<sup>[121]</sup> As shown in Figure 7b, the S<sub>8</sub>/Ketjenblack electrode achieved an outstanding capacity of 1600 mAh g<sup>-1</sup> and a high coulombic efficiency close to 99% even at 1.5 E/S ratio.<sup>[121]</sup> All the above was attributed to the high concentration carbonate electrolyte (6 M LiTFSI in EC/DEC), which successfully turned the sulfur speciation pathway from dissolving precipitation to an akin solid–solid biphasic conversion, inhibiting the dissolution of polysulfide but a small part of the dissolved lithium polysulfide reacted with the solvent in the cathode to form a layer of CEI (cathode electrolyte interface). In addition, the high concentration of LiTFSI not only regulated the solvation effect of carbonate solvent, but also reduced the solvent reaction activity and the electrolyte volatilization. As a diluter, hexafluoroisopropyl methylether (HFME) decreased the viscosity of the complex without the participation of ionic solvation.

#### 4.2. Ionic Liquid-Based Electrolyte

Ionic liquid (IL) electrolytes are considered to be safer than commonly used organic solvents as they themselves own low flammability because of being virtually nonvolatile.<sup>[122]</sup> In addition, because the weak Lewis acidic/basic has a poor interactions between the anions and cations as well as Li polysulfides, ionic liquid electrolyte demonstrated a poor solubility of Li polysulfides.<sup>[123]</sup> However, the ionic liquid has higher viscosity than common liquid organic electrolyte, causing a dull charge transfer and mass transport in Li-S batteries, and demonstrating a poor sulfur utilization. In order to solve this issue, many studies have been done to reduce the viscosity of ionic liquid-based electrolytes. 1,1,2,2-Tetrafluoroethyl-2,2,3,3-tetrafluoropropyl ether (TTE) with lower viscosity was selected to be a co-solvent in ionic liquid-based electrolytes for fabricating the functional electrolytes of Li-S batteries, which can help to promote ionic conductivity, modify and stabilize SEI on Li metal, and reduce charge transfer impedance, as well as restrict dissolution and shuttle of polysulfides.<sup>[124]</sup> In addition, Zhang et al.<sup>[125]</sup> found that the synergistic function of the mixed solvent system (DOL and ethyl 1,1,2,2-tetrafluoroethyl ether (ETFE)) not only improved the ion transport and  $\text{Li}^+$  coordination environment in the IL-based electrolytes, but also contributed to the generation of stable SEI with low resistance on the Li anode surface. In addition, as the solvent–IL interaction influences the ionic conductivity and the SEI film thickness, some room-temperature ionic liquids with functional cations, such as 1-methyl-1-propylpyrrolidinium TFSI(MPP), enhanced cycling performance due to the suppression of dendrite formation, polysulfide shuttling, and SEI growth.<sup>[126]</sup> More interestingly, a poly(ionic liquid)-based quasi-solid-state copolymer electrolyte was reported to capture LiPSs strongly via abundant ester groups in butyl acrylate component of copolymer, and electrostatic repulse free-moving negatively charged ions, which alleviated the loss of active materials. Therefore, the assembled battery achieved a high initial capacity (1179 mA h g<sup>-1</sup>) as well as a lasting cycling performance (849 mAh g<sup>-1</sup> after 200 cycles at 0.5 C) (Figure 7e).<sup>[127]</sup>

#### 4.3. Solid-State Electrolyte

Due to the higher ion conductivity, liquid electrolytes have been extensively adopted for LSBs, but they still go through critical safety risks and

cyclic instability issues, limiting the commercial applications.<sup>[8]</sup> Therefore, in order to solve safety problems, it is an irresistible trend to adopt all-solid-state LSB. The solid-state electrolyte (SSE) should have a wide and stable electrochemical window up to 5 V vs Li/Li<sup>+</sup> as well as an ion conductivity of over  $10^{-3}$  S cm<sup>-1</sup> and, as well as the well compatibility with sulfur cathode and Li anode.<sup>[128]</sup> As shown in Figure 7f, the metal–organic framework (MOF) was employed to modify the gel polymer electrolyte (GPE), which stabilized the lithium anode. The proposed Mg-MOF-74 skeleton with the naturally bifunctional pore structure not only blocked soluble polysulfides from shuttling to the Li anode but also caged Tf<sub>2</sub><sup>-</sup> anions based on the steric hindrance and the Lewis acid-base effect, thereby facilitating a homogeneous flux of Li<sup>+</sup>, which exhibited an excellent cycling life and enhanced rate performance as well as a dense SEI film even after long-term cycles.<sup>[129]</sup> Compared with polymer electrolyte system, the inorganic solid electrolyte system takes more attractive points for LSBs, because of higher safety and lower shuttling effect, as well as higher Li<sup>+</sup> transference number, which benefits regular lithium plating/stripping course and dendrite restriction.<sup>[130,131]</sup> The inorganic solid electrolyte system mainly includes sulfide SEs and oxide SEs. The former owns larger ion radius and higher polarization because of the S<sub>2</sub><sup>-</sup>, which can contribute a higher conductivity, realizing the effective control of interfacial resistance. For example, the all-solid-state lithium–sulfur batteries (ASSLSBs) founded on Li<sub>10</sub>SnP<sub>2</sub>S<sub>12</sub> electrolyte with an excellent ionic conductivity ( $3.2 \times 10^{-3}$  S cm<sup>-1</sup> at RT) delivered a high reversible capacity and superior cyclic performance along with a Coulombic efficiency approaching 100%.<sup>[132]</sup> What's more, there are other innovative efforts. PAN-based double-layer multifunctional gel polymer electrolyte, such as polyacrylonitrile, polyethylene oxide and Li<sub>1.3</sub>Al<sub>0.3</sub>Ti<sub>1.7</sub>(PO<sub>4</sub>)<sub>3</sub> (LATP), offered the high ionic conductivity of PAN while stabilizing Li anode.<sup>[133]</sup>

## 5. Anode

In the past several decades, graphite has dominated the negative electrode of commercial lithium-ion batteries. However, as the growing demand of higher energy densities, graphite has been gradually unable to meet the market needs.<sup>[134,135]</sup> In this context, lithium metal as a kind of anode which has been used before is back in people's sights, especially at the moment of developing lithium–sulfur batteries reported by Nazar in 2009.<sup>[134]</sup> Lithium metal anode has two absolute advantages. For one thing, it provides excellent properties including high theoretical specific capacity (3680 mAh g<sup>-1</sup>) and satisfactory negative redox potential ( $-3.04$  V vs. SHE). For another, metallic lithium plays a role as a lithium source to pair with Li-free cathodes, such as sulfur and fluoride.<sup>[14,136–141]</sup> However, the ultralow reaction potential and ultra-high reactive activation of lithium result in a lot of issues, mainly including the growth of dendrite, the destruction of solid electrolyte interphase (SEI), the anode pulverization, and the dead lithium formation, which are listed in the order in Figure 8.

Since the Fermi level of lithium anode is higher than the low unoccupied molecular orbital of almost all liquid electrolytes,<sup>[142,143]</sup> SEI will be immediately formed once Li anode contacts with the electrolyte (Figure 8). Because the SEI components depend on electrodes, solvents, electrolyte salts, as well as the working status of cells, there is no identical SEI film in two diverse situations.<sup>[144]</sup> Generally, SEI mainly consists of organic species and inorganic components.<sup>[144–146]</sup> In the first discharge and charge process, Li<sup>+</sup> will plating/stripping the anode across

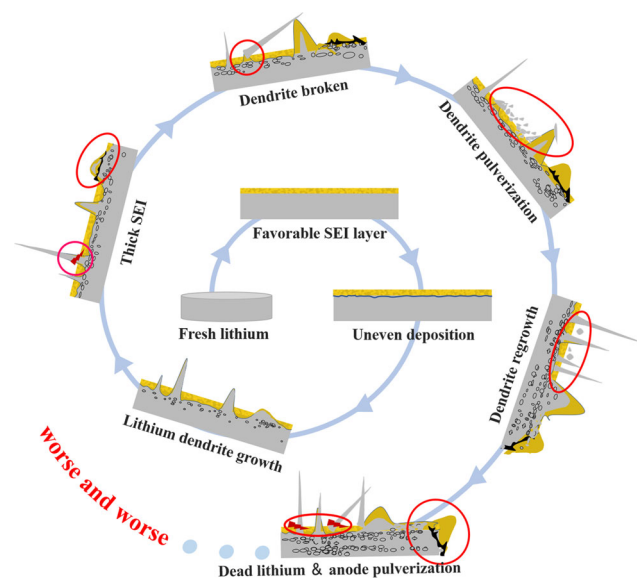


**Figure 8.** The main problems and failure mechanism of lithium metal anode in Li-S batteries. Once the lithium ions do not deposit uniformly, lithium dendrite will grow rapidly, then SEI destruction, dendrite broken and pulverization, dead lithium, anode pulverization, and volumetric change will occur successively.

SEI, at the meantime, a series of polysulfides dissolve in electrolyte and shuttle across separator to Li metal surface. Because of the side reaction between polysulfides and metallic Li, a passivation layer will form, leading to a slow reaction kinetics, a large polarization, and uneven deposition of lithium. Under the influence of the rupture of SEI film, concentration polarization, and uneven distribution of current density, the uneven hills on the anode surface evolve into lithium dendrites.<sup>[147]</sup> Once dendrite, a kind of metal lithium with large specific area contacts with electrolyte, a new but thick SEI film will form. It is suggested that the foot of the lithium dendrites is easier to lose lithium as the dendrite lithium possesses higher reactivity than plate lithium, thus the whole of dendrite breaks at the foot and then pulverizes on the anode surface, forming dead Li wrapped by thick SEI.<sup>[148]</sup> The pulverized dendrites will become new dominant deposition sites, leading to the regrowth of dendrites. At the final, as the cycle number increases the lithium deposition becomes more and more uneven, which in turn increases the dendrite and dead lithium formation, the anode pulverization, and the issues caused by volumetric change (Figure 8).

For the sake of solving these mentioned problems, the modification of lithium anode has received great attention. According to the advances reported so far, studies mainly focus on surface modification, structure architecture, and composition design especially referring to the alloy anode.

### 5.1. Surface Modification

The formation of surface modifications mainly includes in situ and ex situ methods. In situ formation means the SEI is produced during cycles via adding electrolyte additives, which include inorganic salts such as LiNO<sub>3</sub>,<sup>[149]</sup> HF,<sup>[150]</sup> K<sub>4</sub>Bil<sub>7</sub>,<sup>[151]</sup> SOCl<sub>2</sub>,<sup>[152]</sup> La(NO<sub>3</sub>)<sub>3</sub>,<sup>[153]</sup> and P<sub>2</sub>S<sub>5</sub>,<sup>[154]</sup> and organic additives such as diphenyl disulfide (DPDS),<sup>[155]</sup> poly(sulfur-random-1,3-diisopropenylbenzene),<sup>[156]</sup> and 3,5-bis(trifluoromethyl)

thiophenol.<sup>[98]</sup> Tu et al.<sup>[157]</sup> added 0.01 M potassium hexafluorophosphate (KPF<sub>6</sub>) into the 2 M LiTFSI/ether-based electrolyte, resulting in enhanced cycling stability of Li-S batteries. Because of the shield effect of K<sup>+</sup> cation along with the LiF-rich SEI derived from PF<sub>6</sub><sup>-</sup> anions, the Li-S full cell showed excellent performance with a 1210 mAh g<sup>-1</sup> initial value and a 942 mAh g<sup>-1</sup> high capacity at 100th cycle. Jiang et al.<sup>[158]</sup> prepared nitrofullerene (nitro-C<sub>60</sub>) as a bifunctional additive that induced a homogeneous distribution of Li ions and production of NO<sup>2</sup> anions (Figure 9a). As a result, a compact and stable SEI was successfully built, demonstrating markedly improved cycle stability and capacity retention.<sup>[158]</sup> Ex situ formation refers to that SEI was formed before cycle, which mainly involved artificial SEI on the covering of fresh lithium metal anode. There are a great number of means to construct artificial SEI, such as a facile gas/solid reaction,<sup>[159]</sup> liquid/solid reaction,<sup>[160,161]</sup> coating,<sup>[162]</sup> molecular layer deposition (MLD),<sup>[163]</sup> atomic layer deposition (ALD),<sup>[164]</sup> pre-prepared protection layer,<sup>[165–167]</sup> controlled electrochemical method,<sup>[168]</sup> chemical bonds<sup>[169]</sup> and so on. Zhang et al.<sup>[170]</sup> reported a dual-layered artificial SEI that was consisted of organic lithiated Nafion and inorganic Li<sub>x</sub>SiS<sub>y</sub> (Figure 9b), which exhibited higher rate performance (789 mAh g<sup>-1</sup> at 2.0 C) and superior cycling stability (783 mAh g<sup>-1</sup> at 0.5 C after 300 cycles). Compared with SEI formed in situ, the methods of forming SEI by ex situ methods are much more complicated, thus adding additives may be the most promising approach to modify the surface of Li anode and to be widely used in practical application.

## 5.2. Li Host and Current Collector

Structure design that involves host and collector is one of the most important directions to achieve ideal Li anodes. Encapsulating metallic lithium in a porous matrix can effectively avoid the issues such as the irregular lithium deposition, serious volumetric change, and safety threats.<sup>[171]</sup> Present studies about anode host mainly focus on the following materials: 1) porous carbon host including graphene,<sup>[171,172]</sup> carbon fibers (CF),<sup>[173–175]</sup> and covalent organic framework (COF);<sup>[176]</sup> 2) biomass carbon with unique hierarchical geometry, specific chemical affinity, and excellent economy;<sup>[177–180]</sup> 3) A composite of carbon and other materials like nitride, metal element, metal oxide, and MXene.<sup>[97,172,181,182]</sup> It is worth noting that adding nitrogen and silver to the host can largely improve the lithophilic ability of materials. Zhang et al.<sup>[173]</sup> proposed a coralloid silver-coated carbon fiber compound Li anode (CF/Ag-Li) through Ag electropainting and molten Li infusion (Figure 9c). The CF/Ag-Li|Li symmetrical cells could operate at 10.0 mA cm<sup>-2</sup> for 160 cycles, and the produced CF/Ag-Li|S cells exhibited a large capacity retention of 64.3% at 400th cycle.<sup>[173]</sup> It is interesting that some of the host mentioned above can be used as both anode and cathode host.<sup>[183–186]</sup> Manthiram et al.<sup>[183]</sup> prepared a 3D framework coupling lithophilic and catalytic CoSe nanoparticles with conductive carbon nanowires (CoSe@C) as an efficient host both for sulfur and lithium metal, which led to an ultralong lifespan of more than 3000 h with an ultralow overpotential of smaller than 3 mV, and exhibited long lifespan over 600 cycles with a capacity of 5.8 mAh cm<sup>-2</sup>.

As another kind of promising modification method, design of free-standing collectors has become one of the most attractive directions in recent years, which mainly contains three major categories that are carbon, metal, and their compounds.<sup>[138,187]</sup> Carbon collectors consisting of CNTs,<sup>[188,189]</sup> graphene,<sup>[190]</sup> and CNFs<sup>[191–194]</sup> are designed to improve electric conductivity and lead to a homogeneous current

density. Metal collector, especially 3D copper current collector, is the most promising material to commercialize.<sup>[195–198]</sup> Feng et al.<sup>[198]</sup> utilized an one-step facile vacuum distillation approach to fabricate the 3D porous copper current collector from brass foil (Cu-Zn alloy), which showed a steady Coulombic efficiency together with a long lifetime of 800 h in symmetric cells (Figure 9d). In order to achieve both high electrical conductivity and strong lithium affinity, the combination use of carbon and metal was employed. Chen et al.<sup>[194]</sup> designed a 3D structure of a carbon nanofiber (VACNF) array with a planar Cu current collector (VACNF/Cu), delivering a superior cycling stability without any capacity fading after 600 cycles.

## 5.3. Alloy

In order to defend Li metal anode against the parasitic reactions, huge volume change, and dendrite growth, alloy anodes have become one of the most useful methods to modify Li anodes.<sup>[199]</sup> There are a series of alloys (Li<sub>x</sub>M, M = Sn, Al, Sb, B, or Si)<sup>[200,201]</sup> used as anodes. For example, Yushin et al.<sup>[202]</sup> prepared a Li-Al alloy film coated on Li foil as the anode of Li-S batteries, which showed better rate capability, smaller charge transport resistance, and towering Coulombic efficiency. Furthermore, Xia et al.<sup>[139]</sup> found that a conformal thin layer of Sn coated on Li metal surface significantly improved cycle stability with a 99.5% Coulombic efficiency at 500th cycle (Figure 9e). Besides, Gao et al.<sup>[203]</sup> investigated a Li-rich lithium-magnesium (Li-Mg) alloy as the anode of Li-S batteries, in which the robust protection layer was built on the covering of the Li-Mg alloy. As a result, the SEI with smooth morphology formed on Li-Mg alloy efficiently reduced side reactions at the interface. Although many modification methods have been proposed, only using one method cannot achieve an overall improvement in all aspects, even brings up some other problems. Therefore, combining a variety of modification methods could be an ideal mean to improve the comprehensive performance.<sup>[31,204–206]</sup> Recently, Xia et al.<sup>[206]</sup> put forward a powerful 3D sponge nickel (SN) skeleton plus in situ surface engineering strategy to construct a Li/SN anode with a LiF-Li<sub>3</sub>N-rich SEI layer formed by spray quenching, which exhibited a steady overpotential within 75 mV for 1500 h at 5 mA cm<sup>-2</sup>/10 mAh cm<sup>-2</sup> in symmetric cells and remarkable cycling capacity with a primary specific discharge capacity of 784.9 mAh g<sup>-1</sup> in full cells (SEI@Li/SN||SC@Ni<sub>3</sub>S<sub>2</sub>/SN).

## 6. Interlayer and Binder

Apart from designs of cathode, anode, and electrolyte, functional interlayer and binder have been largely developed for strengthening the electrochemical properties of Li-S batteries.<sup>[207]</sup> According to previous studies, various functional interlayers have been designed to inhibit the shuttle of polysulfides, delivering a high Coulombic efficiency and long cycle life.<sup>[208–210]</sup> Recently, metal-organic framework-based separator,<sup>[11]</sup> double-layered separator,<sup>[211]</sup> and composite separator like MoS<sub>2</sub>/Celgard<sup>[212]</sup> have been applied to deliver high-capacity retention and superb cyclic stability. As another essential component, the binder is responsible for cohering active materials and conductive agents onto the current collector, which guarantees the electrode structural integrity and affects the cycle stability and capacity utilization.<sup>[213,214]</sup> Polyvinylidene fluoride (PVDF) is widely used in various rechargeable battery systems, owing to its high bonding strength and wide electrochemical

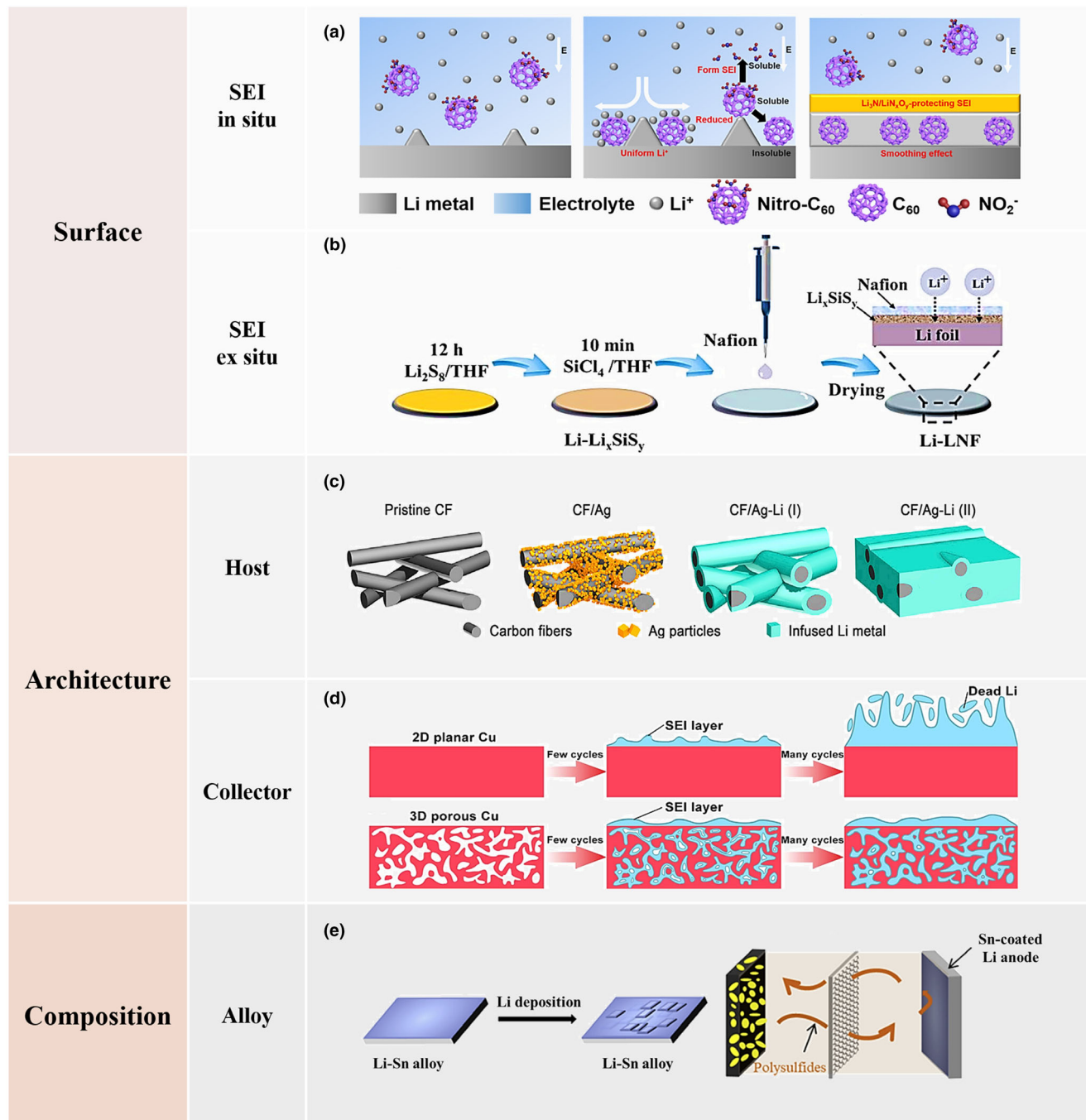


**Figure 9.** The main modification methods of lithium metal anode. a) nitro- $C_60$  as a bifunctional additive to induce SEI in situ; Reproduced with permission.<sup>[158]</sup> Copyright 2019, American Chemical Society. b) dual-layered artificial SEI consisted of organic lithiated Nafion and inorganic  $Li_xSiSy$ ; Reproduced with permission.<sup>[170]</sup> Copyright 2020, Royal Society of Chemistry. c) The process of the coralloid silver-coated carbon fiber-based composite Li anode (CF/Ag-Li); Reproduced with permission.<sup>[173]</sup> Copyright 2018, Elsevier. d) a one-step facile vacuum distillation approach to fabricate the 3D porous Cu current collector; Reproduced with permission.<sup>[198]</sup> Copyright 2018, Elsevier BV. e) The thin Sn layer coating on Li metal surface to suppress the shuttle of polysulfides. Reproduced with permission.<sup>[139]</sup> Copyright 2020, Elsevier.

window. However, it is demonstrated that the PVDF binder can neither keep mechanical stability bringing about swelling and dissolution nor supply sufficient binding to suppress the shuttle effect.<sup>[215]</sup> Furthermore, to maximize the specific energy of Li-S batteries in practical

application, electrodes with high sulfur loading are suggested to be employed, which may cause more serious mechanical problems. Therefore, designing a binder with strong cohesiveness, mechanical stability, and high conductivity both in electric and ionic is of great significance

to enhance the electrochemical property of Li-S batteries. Recently, a bioinspired water-soluble and environmentally friendly binder was synthesized by Zhang et al.,<sup>[216]</sup> reaching a high loading around  $12.0 \text{ mg cm}^{-2}$  and delivering remarkable capacity retention surpass 98% at 1 C even after 300 cycles. Besides improving the performance of the binder, it is also extremely significant to decrease the proportion of total mass for promoting Li-S batteries large-scale utilization. Wang et al.<sup>[217]</sup> only use 0.5 wt. % binder composed with Nafion and PVP to assemble batteries but remained  $970 \text{ mAh g}^{-1}$  at 100th cycle at 0.1 C. Although various binders with different functions and specific structures, such as LiPAA/PVA,<sup>[218]</sup> carbonyl- $\beta$ -cyclodextrin,<sup>[219]</sup> and 3D network binders like TA/PEO<sup>[220]</sup> and P(DAA-r-SBMA-r-PEGMA),<sup>[221]</sup> have been designed to supersede the traditional polyvinylidene fluoride (PVDF) binder, the performance both in chemical and physical is not enough to meet the needs of practical use. Therefore, constructing a kind of binder to solve existing issues is still a nonnegligible task in Li-S batteries.

## 7. Practical Application

In the past three decades, Li-ion batteries have captured a major market in portable electronics and automotive applications ascribed to their outstanding performance. However, Li-ion batteries have arrived at their ceiling in gravimetric and volumetric energy density and cannot satisfy the intense market demand. Fortunately, compared with commercially Li-ion batteries, Li-S batteries are extensively investigated due to the extremely high theoretical energy density and the world-wide abundance of sulfur as cathode active materials.<sup>[222]</sup> As a promising candidate, Li-S batteries overcome energy density limitations of common lithium-ion batteries and would be hopeful to replace Li-ion batteries in high specific energy fields.<sup>[223–225]</sup> Nevertheless, most of the studies focused on Li-S coin cells instead of pouch cells that are closer to practical applications, and several studies have already proved that there are huge gaps between the coin cells and pouch cells in terms of chemical reaction process and failure mechanism.<sup>[226,227]</sup> In this section, we mainly discuss the present problems, solutions, and application scenarios toward the practical application of Li-S pouch cells.

Different from coin cells assembled in the laboratory, pouch cells consist of a great number of pole pieces with abundant active materials gathered by lamination process, resulting in lots of intractable problems while greatly decreased battery capacity.<sup>[228]</sup> Firstly, there is serious electrolyte consumption due to the dendrites or dead Li formation as well as the crack reformation of the SEI layer during cycling.<sup>[171]</sup> Secondly, rather poor reaction kinetics under the thick sulfur cathode and lean electrolyte condition severely limits the capacity utilization of sulfur. Numerous sulfur molecules participating in the Li-S conversion reaction during charging and discharging processes increase the “shuttle effect,” which gives rise to severe capacity damping and low Coulombic efficiency.<sup>[229]</sup> Thirdly, when the overcharge voltage rises to about 4.2V, the battery temperature rises rapidly and the electrolyte oxidizes. The accumulation of heat inside cell results in the decompositions of electrolyte and active materials which will inevitably lead to the thermal runaway.<sup>[230]</sup> In addition, it is suggested that Li metal powdering and the induced polarization caused by Li dendrite and dead lithium are more responsible for pouch cells failure in comparison with LiPSs shuttle issue.<sup>[227,230,231]</sup>

To date, various solutions have been explored to solve the problems mentioned above, such as electrolyte modification, electrode

materials modulation, and functional materials like flame retardant addition.<sup>[17,232]</sup> It seems that electrolyte modification is the most convenient and efficient mean to improve the performance of cells either in coin or pouch cells. An optimized solution to suppress shuttle effect and to form a stable SEI is that adding LiNO<sub>3</sub> to the electrolyte.<sup>[233,234]</sup> So far, the commercialization of Li-S batteries faces many challenges. As exhibited in Figure 10, Li-S pouch cells used in practical applications not only need favorable cycle stability and high Coulombic efficiency but also demand high specific energy both in gravimetric and volumetric. Therefore, it is extremely significant to maximize active materials but minimize electrolyte and other inert matter. Zhao et al.<sup>[15]</sup> demonstrated an enduring Li-Se/S pouch cell with a S loading of  $4.5 \text{ mg cm}^{-2}$ , a lean electrolyte/sulfur ratio about  $10 \mu\text{L mg}^{-1}$  as well as fast redox kinetics, which achieved a high primary specific capacity of  $1312 \text{ mAh g}^{-1}$  at  $0.2 \text{ A g}^{-1}$ . Besides cycle stability and specific energy, safety reliability is also an essential evaluation indicator considering the natural flammability property of sulfur and electrolyte. Monisha et al.<sup>[232]</sup> prepared a suitable and safe cathode material covalently linked sulfur flame retarding copolymer that provided a novel strategy to realize the integrated preparation of active materials and flame retardant functional additives. As for actual application scenarios, Li-S batteries most likely to be applied in some specific-need fields that require high power with low mass but are

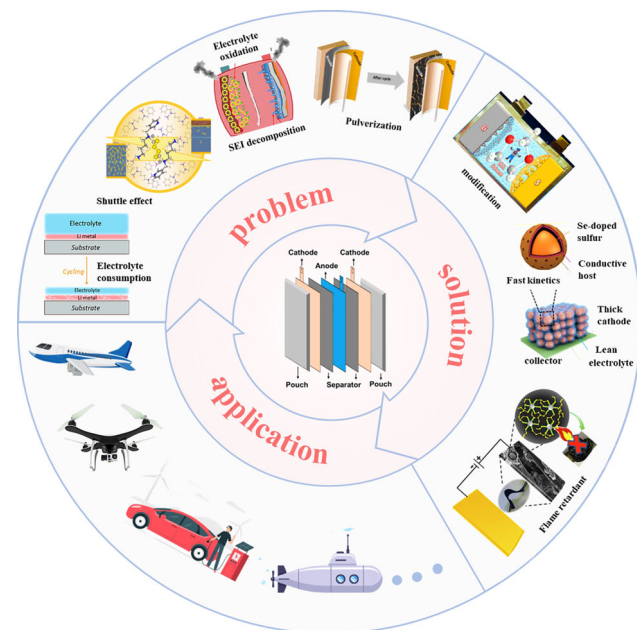


**Figure 10.** Problems, solutions, and applications of Li-S pouch cells. The problems of pouch cells mainly focus on electrolyte consumption,<sup>[171]</sup> Reproduced with permission.<sup>[229]</sup> Copyright 2020, American Chemical Society. Shuttle effect, Reproduced with permission.<sup>[229]</sup> Copyright 2020, American Chemical Society. Electrolyte oxidation and SEI decomposition, Reproduced with permission.<sup>[230]</sup> Copyright 2020, Elsevier. And anode pulverization; Reproduced with permission.<sup>[227]</sup> Copyright 2017, Elsevier. The main solutions including electrolyte modification, Reproduced with permission.<sup>[235]</sup> Copyright 2017, Elsevier BV. Functional additives like flame retardant, Reproduced with permission.<sup>[232]</sup> Copyright 2020, Elsevier. Loading increase and kinetics improvement; Reproduced with permission.<sup>[15]</sup> Copyright 2020, John Wiley and Sons Ltd. the applications involve unmanned aerial vehicles (UAVs), cargo aircraft, electric vehicles, and submarines, etc.

less concerned about cycle life.<sup>[223]</sup> The most well-known application is unmanned aerial vehicles (UAVs) that long to minimize the mass of fuselage for longer range. Moreover, cargo aircraft, electric vehicles especially heavy automotive vehicles, submarines, space sectors, and portable devices are likely to be the suitable avenue bringing Li-S batteries to market with an extremely high performance.

## 8. Summary and Outlook

This review illustrates the working principle and remaining challenges of Li-S batteries and retrospect the most recent advances in the cathode, electrolyte, anode, binder, and practical applications. As for cathode, two strategies to anchor the long-chain polysulfides have been considered, including physical constraints and chemical bonds. Four different types of sulfur host materials, including carbon materials, polar inorganic materials, organosulfur compounds, and flexible sulfur cathodes, have been discussed with the target of limiting the diffusion of polysulfides. For the electrolyte part, this article mainly reviews the recent progress in exploiting lean electrolyte in Li-S batteries. When the amount of electrolyte decreases, for traditional liquid electrolytes, the problems of increased battery polarization and decreased cycle stability will occur; for ionic liquid electrolytes and solid electrolytes, problems such as low sulfur utilization and low ion conductivity will occur. After illuminating the main problems and failure mechanism of the lithium metal anode, this review retrospect three modification methods, surface modification, structure design, and composition. Toward the practical application of Li-S pouch cells, the present problems including electrolyte consumption, shuttle effect, SEI decomposition, and anode pulverization are discussed. The solutions focus on electrolyte modification, functional additives like flame retardant, loading increase and kinetics improvement, and some common application scenarios are recommended.

Although the problems like the shuttle of lithium polysulfides, lithium anode dendrite, and volume change have been effectively contained by various modification means, there is still a lengthy way to go before applying on a large scale. To realize the lithium–sulfur batteries wholesale utilization, the following aspects are crucial:

1 Decipher the reaction mechanisms. Though lots of works have been published, the mechanism behind the reaction has not been revealed due to the complicated multistage process, thus only when the reaction mechanism is clear, can the problems of lithium–sulfur batteries be solved fundamentally. Firstly, after fully understand the interaction mechanism between host materials and polysulfides, the exploring of host material with an adsorption–catalysis synergistic effect are rather important. The active sulfur species will be converted into soluble polysulfide during the cycle, so the sulfur host material must limit the polysulfide in the cathode side, and if the host material also shows high electrocatalytic activation for the conversion of active sulfur species, it will increase the utilization rate of sulfur and the electrochemical performance of Li-S batteries. Secondly, studies of lithium–sulfur chemistry under the condition of lean electrolyte should be strengthened. To be specific, the battery performance can be improved by deploying solvent systems, including the application of fluorinated ethers, ionic liquids, and other new solvents, developing functional additives to solve the irreversible active materials loss and lithium dendrites germination, studying

the influence of electrolyte concentration on the electrochemical reaction mechanism of lithium–sulfur batteries. Finally, for understanding the failure mechanism of the lithium anode, factors such as polysulfide and solvation structure should be considered comprehensively. Emphasis should be placed on the study of anode modifications under practical conditions like low negative/positive ratio ( $N/P < 2$ ) and low E/S ratio ( $< 10 \mu\text{L mg}^{-1}$ ).

- 2 Improve materials and technologies. As for materials, active sulfur species content in cathode materials plays an important role. A high energy density can be ensured only when the content of electroactive species is kept high enough. Therefore, it is critical to reduce the content of host material in sulfur cathodes. As for technologies, changing the physical and chemical characterization of materials can effectively reduce the difficulty of the reaction and improve electrochemical performance of batteries. In addition, battery manufacturing technology should be further explored to promote the commercialization of Li-S batteries.
- 3 Stipulate key parameters and configure application systems. Reasonable charge–discharge systems are beneficial to the development of the charge–discharge performances of larger current density to a small extent. In addition, pressure and temperature range used, storage condition, and even dimensions and shape of batteries should be explicitly stipulated. In order to monitor, manage, and protect the battery, it is necessary to develop battery management systems like ECMS (electrical circuit models) and BMS (battery management system) to accurate some key parameters like temperature, state-of-charge (SOC), state-of-health (SOH), and current to estimate the electrochemical property of Li-S batteries. Furthermore, recycling spent batteries is greatly significant to achieve comprehensive utilization of batteries, which should be paid more attention both for resource and environment.

## Acknowledgements

The authors gratefully acknowledge the Innovation-Driven Project of Central South University (No.2019CX033) and the National Natural Science Foundation of China (No. 51904344). R.D, M.W, and H.Y. contributed equally to this work

## Conflict of Interest

The authors declare no conflict of interest.

## Keywords

battery, conversion, high energy density, lithium, sulfur cathode

Received: June 2, 2021

Revised: July 28, 2021

Published online: July 30, 2021

- 
- [1] M. Armand, J.-M. Tarascon, *Nature* **2008**, 451, 652.
  - [2] B. K. Sovacool, R. J. Heffron, D. McCauley, A. Goldthau, *Nat. Energy* **2016**, 1, 1.
  - [3] M. R. Palacín, A. de Guibert, *Science* **2016**, 351, 1253292.
  - [4] X.-B. Cheng, R. Zhang, C.-Z. Zhao, Q. Zhang, *Chem. Rev.* **2017**, 117, 10403.

- [5] F. Wu, J. Maier, Y. Yu, *Chem. Soc. Rev.* **2020**, 49, 1569.
- [6] F. Wu, V. Srot, S. Chen, S. Lerger, P. A. van Aken, J. Maier, Y. Yu, *Adv. Mater.* **2019**, 31, 1905146.
- [7] F. Wu, G. Yushin, *Energy Environ. Sci.* **2017**, 10, 435.
- [8] B. Liu, R. Fang, D. Xie, W. Zhang, H. Huang, Y. Xia, X. Wang, X. Xia, J. Tu, *Energy Environ. Mater.* **2018**, 1, 196.
- [9] C. Yang, P. Li, J. Yu, L.-D. Zhao, L. Kong, *Energy* **2020**, 201, 117718.
- [10] Q. Pang, X. Liang, C. Y. Kwok, L. F. Nazar, *Nat. Energy* **2016**, 1, 16132.
- [11] F. Wu, J. T. Lee, Y. Xiao, G. Yushin, *Nano Energy* **2016**, 27, 238.
- [12] Y. X. Yin, S. Xin, Y. G. Guo, L. J. Wan, *Angew. Chem. Int. Ed.* **2013**, 52, 13186.
- [13] M. Zhao, B. Q. Li, H. J. Peng, H. Yuan, J. Y. Wei, J. Q. Huang, *Angew. Chem. Int. Ed.* **2020**, 59, 12636.
- [14] L.-P. Hou, X.-Q. Zhang, B.-Q. Li, Q. Zhang, *Mater. Today* **2021**, 45, 62.
- [15] C. Zhao, G. L. Xu, T. Zhao, K. Amine, *Angew. Chem. Int. Ed.* **2020**, 59, 17634.
- [16] S. Dörfler, H. Althues, P. Härtel, T. Abendroth, B. Schumm, S. Kaskel, *Joule* **2020**, 4, 539.
- [17] J. Wang, F. Lin, H. Jia, J. Yang, C. W. Monroe, Y. NuLi, *Angew. Chem. Int. Ed.* **2014**, 53, 10099.
- [18] Y. Lin, J. Zheng, C. Wang, Y. Qi, *Nano Energy* **2020**, 75, 104915.
- [19] S. Luo, F. Wu, G. Yushin, *Mater. Today* **2021**. In press. Doi: <https://doi.org/10.1016/j.mattod.2021.03.017>
- [20] G. R. Li, S. Wang, Y. N. Zhang, M. Li, Z. W. Chen, J. Lu, *Adv. Mater.* **2018**, 30, 19.
- [21] X. Ji, K. T. Lee, L. F. Nazar, *Nat. Mater.* **2009**, 8, 500.
- [22] Y. Yang, G. Yu, J. J. Cha, H. Wu, M. Vosgueritchian, Y. Yao, Z. Bao, Y. Cui, *ACS Nano* **2011**, 5, 9187.
- [23] X. Liu, J.-Q. Huang, Q. Zhang, L. Mai, *Adv. Mater.* **2017**, 29, 1601759.
- [24] Q. Pang, C. Y. Kwok, D. Kundu, X. Liang, L. F. Nazar, *Joule* **2019**, 3, 136.
- [25] J. Li, J. Wu, T. Zhang, L. Huang, *Acta Phys. -Chim. Sin.* **2017**, 33, 968.
- [26] J. Liang, Z.-H. Sun, F. Li, H.-M. Cheng, *Energy Storage Mater.* **2016**, 2, 76.
- [27] Z. Li, Y. Huang, L. Yuan, Z. Hao, Y. Huang, *Carbon* **2015**, 92, 41.
- [28] C. Chen, D. Li, L. Gao, P. P. R. M. L. Harks, R. A. Eichel, P. H. L. Notten, *J. Mater. Chem. A* **2017**, 5, 1428.
- [29] R. Yan, M. Oschatz, F. Wu, *Carbon* **2020**, 161, 162.
- [30] F. Wu, S. Thieme, A. Ramanujapuram, E. Zhao, C. Weller, H. Althues, S. Kaskel, O. Borodin, G. Yushin, *Nano Energy* **2017**, 40, 170.
- [31] Q. Dong, B. Hong, H. Fan, H. Jiang, K. Zhang, Y. Lai, *ACS Appl. Mater. Interfaces* **2020**, 12, 627.
- [32] S. Xin, L. Gu, N.-H. Zhao, Y.-X. Yin, L.-J. Zhou, Y.-G. Guo, L.-J. Wan, *J. Am. Chem. Soc.* **2012**, 134, 18510.
- [33] Z. Li, L. Yuan, Z. Yi, Y. Sun, Y. Liu, Y. Jiang, Y. Shen, Y. Xin, Z. Zhang, Y. Huang, *Adv. Energy Mater.* **2014**, 4, 1301473.
- [34] Y. Li, I. A. Murphy, Y. Chen, F. Lin, X. Wang, S. Wang, D. Hubble, S. H. Jang, K. T. Muller, C. Wang, A. K. Y. Jen, J. Yang, *J. Mater. Chem. A* **2019**, 7, 13372.
- [35] G. Zheng, Y. Yang, J. J. Cha, S. S. Hong, Y. Cui, *Nano Lett.* **2011**, 11, 4462.
- [36] Y. Zhao, W. Wu, J. Li, Z. Xu, L. Guan, *Adv. Mater.* **2014**, 26, 5113.
- [37] Z. Li, H. B. Wu, X. W. Lou, *Energy Environ. Sci.* **2016**, 9, 3061.
- [38] Z. Yu, M. Liu, D. Guo, J. Wang, X. Chen, J. Li, H. Jin, Z. Yang, X. Chen, S. Wang, *Angew. Chem. Int. Ed.* **2020**, 59, 6406.
- [39] D. Gueon, J. T. Hwang, S. B. Yang, E. Cho, K. Sohn, D. K. Yang, J. H. Moon, *ACS Nano* **2018**, 12, 226.
- [40] G. Shen, Z. Liu, P. Liu, J. Duan, H. A. Younus, H. Deng, X. Wang, S. Zhang, *J. Mater. Chem. A* **2020**, 8, 1154.
- [41] M. Hagen, D. Hanselmann, K. Ahlbrecht, R. Maca, D. Gerber, J. Tuebke, *Adv. Energy Mater.* **2015**, 5, 1401986.
- [42] P. Bonnick, E. Nagai, J. Muldoon, *J. Electrochem. Soc.* **2018**, 165, A6005.
- [43] G. Li, W. Lei, D. Luo, Y. Deng, Z. Deng, D. Wang, A. Yu, Z. Chen, *Energy Environ. Sci.* **2018**, 11, 2372.
- [44] J. H. Yun, J.-H. Kim, D. K. Kim, H.-W. Lee, *Nano Lett.* **2018**, 18, 475.
- [45] Y. Li, X.-T. Guo, S.-T. Zhang, H. Pang, *Rare Met.* **2020**, 40, 417.
- [46] K. Chen, R. Fang, F. Li, H. Cheng, *Acta Phys. -Chim. Sin.* **2018**, 34, 377.
- [47] L. Duan, L. Zhao, H. Cong, X. Zhang, W. Lu, C. Xue, *Small* **2019**, 15, 1804347.
- [48] Y. Li, M. Chen, P. Zeng, H. Liu, H. Yu, Z. Luo, Y. Wang, B. Chang, X. Wang, *J. Alloys Compd.* **2021**, 873, 159883.
- [49] G. Y. Xu, B. Ding, P. Nie, L. F. Shen, J. Wang, X. G. Zhang, *Chem. Eur. J.* **2013**, 19, 12306.
- [50] Q. Pang, D. Kundu, M. Cuisinier, L. F. Nazar, *Nat. Commun.* **2014**, 5, 4759.
- [51] Y. Wang, R. Zhang, J. Chen, H. Wu, S. Lu, K. Wang, H. Li, C. J. Harris, K. Xi, R. V. Kumar, S. Ding, *Adv. Energy Mater.* **2019**, 9, 1900953.
- [52] J. He, L. Luo, Y. Chen, A. Manthiram, *Adv. Mater.* **2017**, 29, 1702707.
- [53] Z. Li, J. Zhang, X. W. Lou, *Angew. Chem. Int. Ed.* **2015**, 54, 12886.
- [54] M. Yu, W. Yuan, C. Li, J.-D. Hong, G. Shi, *J. Mater. Chem. A* **2014**, 2, 7360.
- [55] X. Ji, S. Evers, R. Black, L. F. Nazar, *Nat. Commun.* **2011**, 2, 325.
- [56] Q. Fan, W. Liu, Z. Weng, Y. Sun, H. Wang, *J. Am. Chem. Soc.* **2015**, 137, 12946.
- [57] J. Zhang, P. Gu, J. Xu, H. Xue, H. Pang, *Nanoscale* **2016**, 8, 18578.
- [58] F. Wu, T. Pollard, E. Zhao, Y. Xiao, M. Olguin, O. Borodin, G. Yushin, *Energy Environ. Sci.* **2018**, 11, 807.
- [59] Z. Yuan, H.-J. Peng, T.-Z. Hou, J.-Q. Huang, C.-M. Chen, D.-W. Wang, X.-B. Cheng, F. Wei, Q. Zhang, *Nano Lett.* **2016**, 16, 519.
- [60] Z. W. Seh, J. H. Yu, W. Li, P. C. Hsu, H. Wang, Y. Sun, H. Yao, Q. Zhang, Y. Cui, *Nat. Commun.* **2014**, 5, 5017.
- [61] W. Xue, Z. Shi, L. Suo, C. Wang, Z. Wang, H. Wang, K. P. So, A. Mauzano, D. Yu, Y. Chen, L. Qie, Z. Zhu, G. Xu, J. Kong, J. Li, *Nat. Energy* **2019**, 4, 374.
- [62] H. Wang, Q. Zhang, H. Yao, Z. Liang, H.-W. Lee, P.-C. Hsu, G. Zheng, Y. Cui, *Nano Lett.* **2014**, 14, 7138.
- [63] Y. Lu, X. Li, J. Liang, L. Hu, Y. Zhu, Y. Qian, *Nanoscale* **2016**, 8, 17616.
- [64] S. Zhao, X. Tian, Y. Zhou, B. Ma, A. Natarajan, *J. Energy Chem.* **2020**, 46, 22.
- [65] X. Huang, J. Tang, B. Luo, R. Knibbe, T. Lin, H. Hu, M. Rana, Y. Hu, X. Zhu, Q. Gu, D. Wang, L. Wang, *Adv. Energy Mater.* **2019**, 9, 1901872.
- [66] Z. Cui, C. Zu, W. Zhou, A. Manthiram, J. B. Goodenough, *Adv. Mater.* **2016**, 28, 6926.
- [67] Z. Li, Q. He, X. Xu, Y. Zhao, X. Liu, C. Zhou, D. Ai, L. Xia, L. Mai, *Adv. Mater.* **2018**, 30, 1804089.
- [68] R. Li, H. Peng, Q. Wu, X. Zhou, J. He, H. Shen, M. Yang, C. Li, *Angew. Chem. Int. Ed.* **2020**, 59, 12129.
- [69] Z.-W. Zhang, H.-J. Peng, M. Zhao, J.-Q. Huang, *Adv. Funct. Mater.* **2018**, 28, 1707536.
- [70] M. Naguib, M. Kurtoglu, V. Presser, J. Lu, J. Niu, M. Heon, L. Hultman, Y. Gogotsi, M. W. Barsoum, *Adv. Mater.* **2011**, 23, 4248.
- [71] M. Naguib, O. Mashtalir, J. Carle, V. Presser, J. Lu, L. Hultman, Y. Gogotsi, M. W. Barsoum, *ACS Nano* **2012**, 6, 1322.
- [72] B. Anasori, Y. Xie, M. Beidaghi, J. Lu, B. C. Hosler, L. Hultman, P. R. C. Kent, Y. Gogotsi, M. W. Barsoum, *ACS Nano* **2015**, 9, 9507.
- [73] M. Ghidiu, M. Naguib, C. Shi, O. Mashtalir, L. M. Pan, B. Zhang, J. Yang, Y. Gogotsi, S. J. L. Billinge, M. W. Barsoum, *Chem. Comm.* **2014**, 50, 9517.
- [74] X. Liang, A. Garsuch, L. F. Nazar, *Angew. Chem. Int. Ed.* **2015**, 54, 3907.
- [75] H. Tang, W. Li, L. Pan, C. P. Cullen, Y. Liu, A. Pakdel, D. Long, J. Yang, N. McEvoy, G. S. Duesberg, V. Nicolosi, C. Zhang, *Adv. Sci.* **2018**, 5, 1800502.
- [76] R. Wang, C. Luo, T. Wang, G. Zhou, Y. Deng, Y. He, Q. Zhang, F. Kang, W. Lv, Q. H. Yang, *Adv. Mater.* **2020**, 32, 2000315.
- [77] Y. Wang, F. Chu, J. Zeng, Q. Wang, T. Naren, Y. Li, Y. Cheng, Y. Lei, F. Wu, *ACS Nano* **2021**, 15, 210.
- [78] Z. Liu, L. Zhou, Q. Ge, R. Chen, M. Ni, W. Utetiwabo, X. Zhang, W. Yang, *ACS Appl. Mater. Interfaces* **2018**, 10, 19311.
- [79] Z. Du, X. Chen, W. Hu, C. Chuang, S. Xie, A. Hu, W. Yan, X. Kong, X. Wu, H. Ji, L.-J. Wan, *J. Am. Chem. Soc.* **2019**, 141, 3977.

- [80] G. L. Yuan, J. N. Pan, Y. G. Zhang, J. X. Yu, Y. J. He, Y. Su, Q. Zhou, H. Y. Jin, S. H. Xie, *RSC Adv.* **2018**, 8, 17950.
- [81] F. Wu, H. Lv, S. Chen, S. Lorger, V. Srot, M. Oschatz, P. van Aken, X. Wu, J. Maier, Y. Yu, *Adv. Funct. Mater.* **2019**, 29, 9.
- [82] Y. Liang, Z. Tao, J. Chen, *Adv. Energy Mater.* **2012**, 2, 742.
- [83] S. J. Visco, L. C. DeJonghe, *J. Electrochem. Soc.* **1988**, 135, 12.
- [84] H. Kim, J. Lee, H. Ahn, O. Kim, M. J. Park, *Nat. Commun.* **2015**, 6, 7278.
- [85] F. Wu, S. Chen, V. Srot, Y. Huang, S. K. Sinha, P. A. van Aken, J. Maier, Y. Yu, *Adv. Mater.* **2018**, 30, 1706643.
- [86] J. Wang, J. Yang, J. Xie, N. Xu, *Adv. Mater.* **2002**, 14, 963.
- [87] W. Wang, Z. Cao, G. A. Elia, Y. Wu, W. Wahyudi, E. Abou-Hamad, A.-H. Emwas, L. Cavallo, L.-J. Li, J. Ming, *ACS Energy Lett.* **2018**, 3, 2899.
- [88] X. Chen, L. Peng, L. Wang, J. Yang, Z. Hao, J. Xiang, K. Yuan, Y. Huang, B. Shan, L. Yuan, J. Xie, *Nat. Commun.* **2019**, 10, 1021.
- [89] Y. Cui, J. D. Ackerson, Y. Ma, A. Bhargav, J. A. Karty, W. Guo, L. Zhu, Y. Fu, *Adv. Funct. Mater.* **2018**, 28, 1801791.
- [90] D.-Y. Wang, Y. Si, J. Li, Y. Fu, *J. Mater. Chem. A* **2019**, 7, 7423.
- [91] S. Iijima, *Nature* **1991**, 354, 56.
- [92] J.-H. Kim, Y.-H. Lee, S.-J. Cho, J.-G. Gwon, H. J. Cho, M. Jang, S.-Y. Lee, S.-Y. Lee, *Energy Environ. Sci.* **2019**, 12, 177.
- [93] G. Zhou, L. Li, C. Ma, S. Wang, Y. Shi, N. Koratkar, W. Ren, F. Li, H.-M. Cheng, *Nano Energy* **2015**, 11, 356.
- [94] J. Cao, C. Chen, Q. Zhao, N. Zhang, Q. Lu, X. Wang, Z. Niu, J. Chen, *Adv. Mater.* **2016**, 28, 9629.
- [95] H. Li, H. Chen, Y. Xue, Y. Zhang, M. Zhang, W. Yu, G. Bai, K. Zhuo, Y. Zheng, *Adv. Energy Mater.* **2020**, 10, 2001683.
- [96] Z. Wang, J. Shen, J. Liu, X. Xu, Z. Liu, R. Hu, L. Yang, Y. Feng, Z. Shi, L. Ouyang, Y. Yu, M. Zhu, *Adv. Mater.* **2019**, 31, 1902228.
- [97] S. Liu, J. Li, X. Yan, Q. Su, Y. Lu, J. Qiu, Z. Wang, X. Lin, J. Huang, R. Liu, B. Zheng, L. Chen, R. Fu, D. Wu, *Adv. Mater.* **2018**, 30, 1706895.
- [98] W.-J. Chen, C.-X. Zhao, B.-Q. Li, Q. Jin, X.-Q. Zhang, T.-Q. Yuan, X. Zhang, Z. Jin, S. Kaskel, Q. Zhang, *Energy Environ. Mater.* **2020**, 3, 160.
- [99] S. Yang, X. Xu, X. Cheng, X. Wang, J. Chen, Y. Xiao, H. Yuan, H. Liu, A. Chen, W. Zhu, J. Huang, Q. Zhang, *Acta Phys. -Chim. Sin.* **2021**, 37, 2007058.
- [100] W. Chen, T. Lei, C. Wu, M. Deng, C. Gong, K. Hu, Y. Ma, L. Dai, W. Lv, W. He, X. Liu, J. Xiong, C. Yan, *Adv. Energy Mater.* **2018**, 8, 1702348.
- [101] T. A. Pascal, K. H. Wujcik, D. R. Wang, N. P. Balsara, D. Prendergast, *Phys. Chem. Chem. Phys.* **2017**, 19, 1441.
- [102] R. Glaser, F. Wu, E. Register, M. Tolksdorf, B. Johnson, J. Ready, M. Sanghadasa, G. Yushin, *J. Electrochem. Soc.* **2020**, 167, 100512.
- [103] G.-Y. Du, C.-Y. Liu, E. Y. Li, *Catalysts* **2020**, 10, 911.
- [104] Z. Li, Y. Zhou, Y. Wang, Y.-C. Lu, *Adv. Energy Mater.* **2019**, 9, 1802207.
- [105] M. Zhao, B.-Q. Li, X.-Q. Zhang, J.-Q. Huang, Q. Zhang, *ACS Cent. Sci.* **2020**, 6, 1095.
- [106] F. Y. Fan, Y. M. Chiang, *J. Electrochem. Soc.* **2017**, 164, 4.
- [107] Q. J. Meisner, T. Rojas, N. L. D. Rago, J. Cao, J. Bareño, T. Glossmann, A. Hintennach, P. C. Redfern, D. Pahls, L. Zhang, *J. Power Sources* **2019**, 438, 226939.
- [108] S. Drvarić Talian, S. Jeschke, A. Vizintin, K. Pirnat, I. Arčon, G. Aquilanti, P. Johansson, R. Dominko, *Chem. Mater.* **2017**, 29, 10037.
- [109] J. Zheng, J. A. Lochala, A. Kwok, Z. D. Deng, J. Xiao, *Adv. Sci.* **2017**, 4, 1700032.
- [110] Y. Yamada, K. Furukawa, K. Sodeyama, K. Kikuchi, M. Yaegashi, Y. Tateyama, A. Yamada, *J. Am. Chem. Soc.* **2014**, 136, 5039.
- [111] Y. Yamada, K. Usui, C. H. Chiang, K. Kikuchi, K. Furukawa, A. Yamada, *ACS Appl. Mater. Interfaces* **2014**, 6, 10892.
- [112] K. Sun, N. Li, D. Su, H. Gan, *J. Electrochem. Soc.* **2019**, 166, A50.
- [113] J.-Y. Hwang, H. M. Kim, Y.-K. Sun, *J. Electrochem. Soc.* **2017**, 165, A5006.
- [114] Q. Pang, A. Shyamsunder, B. Narayanan, C. Y. Kwok, L. A. Curtiss, L. F. Nazar, *Nat. Energy* **2018**, 3, 783.
- [115] F. Wu, F. Chu, G. A. Ferrero, M. Sevilla, A. B. Fuertes, O. Borodin, Y. Yu, G. Yushin, *Nano Lett.* **2020**, 20, 5391.
- [116] J. Zhou, Y. Guo, C. Liang, L. Cao, H. Pan, J. Yang, J. Wang, *Chem. Comm.* **2018**, 54, 5478.
- [117] A. Shyamsunder, W. Beichel, P. Klose, Q. Pang, H. Scherer, A. Hoffmann, G. K. Murphy, I. Krossing, L. F. Nazar, *Angew. Chem. Int. Ed.* **2017**, 56, 6192.
- [118] J. Gao, M. A. Lowe, Y. Kiya, H. D. Abruna, *J. Phys. Chem. C* **2011**, 115, 25132.
- [119] S. Warneke, A. Hintennach, M. R. Buchmeiser, *J. Electrochem. Soc.* **2018**, 165, A2093.
- [120] F. Wu, C. Zhao, S. Chen, Y. Lu, Y. Hou, Y.-S. Hu, J. Maier, Y. Yu, *Mater. Today* **2018**, 21, 960.
- [121] F. Huang, L. Gao, Y. Zou, G. Ma, J. Zhang, S. Xu, Z. Li, X. Liang, J. Mater. Chem. A **2019**, 7, 12498.
- [122] K. Dokko, N. Tachikawa, K. Yamauchi, M. Tsuchiya, A. Yamazaki, E. Takashima, J.-W. Park, K. Ueno, S. Seki, N. Serizawa, M. Watanabe, *J. Electrochem. Soc.* **2013**, 160, A1304.
- [123] J. W. Park, K. Ueno, N. Tachikawa, K. Dokko, M. Watanabe, *J. Phys. Chem. C* **2013**, 117, 20531.
- [124] H. Lu, Z. Chen, H. Du, K. Zhang, J. Wang, Z. Hou, J. Fang, *Ionics* **2019**, 25, 2685.
- [125] H. Lu, Y. Zhu, B. Zheng, H. Du, X. Zheng, C. Liu, Y. Yuan, J. Fang, K. Zhang, *New J. Chem.* **2020**, 44, 361.
- [126] S. Suriyakumar, M. Kathiresan, A. M. Stephan, *ACS Omega* **2019**, 4, 3894.
- [127] X. Cai, B. Cui, B. Ye, W. Wang, J. Ding, G. Wang, *ACS Appl. Mater. Interfaces* **2019**, 11, 38136.
- [128] M. R. Busche, D. A. Weber, Y. Schneider, C. Dietrich, S. Wenzel, T. Leichtweiss, D. Schröder, W. Zhang, H. Weigand, D. Walter, S. J. Sedlmaier, D. Houtarde, L. F. Nazar, J. Janek, *Chem. Mater.* **2016**, 28, 6152.
- [129] D.-D. Han, Z.-Y. Wang, G.-L. Pan, X.-P. Gao, *ACS Appl. Mater. Interfaces* **2019**, 11, 18427.
- [130] Y. Liu, P. He, H. Zhou, *Adv. Energy Mater.* **2018**, 8, 1701602.
- [131] Y.-Z. Sun, J.-Q. Huang, C.-Z. Zhao, Q. Zhang, *Sci. China Chem.* **2017**, 60, 1508.
- [132] J. Yi, L. Chen, Y. Liu, H. Geng, L.-Z. Fan, *ACS Appl. Mater. Interfaces* **2019**, 11, 36774.
- [133] X. Wang, X. Hao, Y. Xia, Y. Liang, X. Xia, J. Tu, *J. Membr. Sci.* **2019**, 582, 37.
- [134] Y. P. Wu, E. Rahm, R. Holze, *J. Power Sources* **2003**, 114, 228.
- [135] V. Aravindan, Y. S. Lee, S. Madhavi, *Adv. Energy Mater.* **2015**, 5, 43.
- [136] W. Xu, J. L. Wang, F. Ding, X. L. Chen, E. Nasibutin, Y. H. Zhang, J. G. Zhang, *Energy Environ. Sci.* **2014**, 7, 513.
- [137] R. Wang, W. Cui, F. Chu, F. Wu, *J. Energy Chem.* **2020**, 48, 145.
- [138] H. Zhao, N. Deng, J. Yan, W. Kang, J. Ju, Y. Ruan, X. Wang, X. Zhuang, Q. Li, B. Cheng, *Chem. Eng. J.* **2018**, 347, 343.
- [139] S. Xia, X. Zhang, C. Liang, Y. Yu, W. Liu, *Energy Storage Mater.* **2020**, 24, 329.
- [140] M. Zhao, X. Chen, X.-Y. Li, B.-Q. Li, J.-Q. Huang, *Adv. Mater.* **2021**, 33, 2007298.
- [141] F. Liu, Z. Zhang, S. Ye, Y. Yao, Y. Yu, *Acta Phys. -Chim. Sin.* **2021**, 37, 2006021.
- [142] M. Wang, Z. Peng, W. Luo, Q. Zhang, Z. Li, Y. Zhu, H. Lin, L. Cai, X. Yao, C. Ouyang, D. Wang, *Adv. Sci.* **2020**, 7, 2000237.
- [143] Y.-X. Yin, H.-R. Yao, Y.-G. Guo, *Chin. Phys. B* **2016**, 25, 18801.
- [144] X. B. Cheng, R. Zhang, C. Z. Zhao, F. Wei, J. G. Zhang, Q. Zhang, *Adv. Sci.* **2016**, 3, 1500213.
- [145] S. Xiong, K. Xie, Y. Diao, X. Hong, *J. Power Sources* **2014**, 246, 840.
- [146] L. Wang, Y. Lin, S. DeCarlo, Y. Wang, K. Leung, Y. Qi, K. Xu, C. Wang, B. W. Eichhorn, *Chem. Mater.* **2020**, 32, 3765.
- [147] Y. Luo, L. Guo, M. Xiao, S. Wang, S. Ren, D. Han, Y. Meng, *J. Mater. Chem. A* **2020**, 8, 4629.

- [148] X. Xu, S. Wang, H. Wang, B. Xu, C. Hu, Y. Jin, J. Liu, H. Yan, *J. Energy Storage* **2017**, 13, 387.
- [149] Z. W. Seh, Y. Sun, Q. Zhang, Y. Cui, *Chem. Soc. Rev.* **2016**, 45, 5605.
- [150] K. Kanamura, S. Shiraishi, Z. Takehara, *J. Electrochem. Soc.* **1996**, 143, 2187.
- [151] Y. Cui, S. Liu, B. Liu, D. Wang, Y. Zhong, X. Zhang, X. Wang, X. Xia, C. Gu, J. Tu, *Front. Chem.* **2019**, 7, 952.
- [152] S. Li, H. Dai, Y. Li, C. Lai, J. Wang, F. Huo, C. Wang, *Energy Storage Mater.* **2019**, 18, 222.
- [153] S. Liu, G. R. Li, X. P. Gao, *ACS Appl. Mater. Interfaces* **2016**, 8, 7783.
- [154] Z. Lin, Z. Liu, W. Fu, N. J. Dudney, C. Liang, *Adv. Funct. Mater.* **2013**, 23, 1064.
- [155] X. Yan, H. Zhang, M. Huang, M. Qu, Z. Wei, *Chemsuschem* **2019**, 12, 2263.
- [156] G. Li, Q. Huang, X. He, Y. Gao, D. Wang, S. H. Kim, D. Wang, *ACS Nano* **2018**, 12, 1500.
- [157] J. Li, S. Liu, Y. Cui, S. Zhang, X. Wu, J. Xiang, M. Li, X. Wang, X. Xia, C. Gu, J. Tu, *ACS Appl. Mater. Interfaces* **2020**, 12, 56017.
- [158] Z. Jiang, Z. Zeng, C. Yang, Z. Han, W. Hu, J. Lu, J. Xie, *Nano Lett.* **2019**, 19, 8780.
- [159] F. Liu, L. Wang, Z. Zhang, P. Shi, Y. Feng, Y. Yao, S. Ye, H. Wang, X. Wu, Y. Yu, *Adv. Funct. Mater.* **2020**, 30, 2001607.
- [160] Y. X. Yao, X. Q. Zhang, B. Q. Li, C. Yan, P. Y. Chen, J. Q. Huang, Q. Zhang, *InfoMat* **2020**, 2, 379.
- [161] Y. Lu, S. Gu, X. Hong, K. Rui, X. Huang, J. Jin, C. Chen, J. Yang, Z. Wen, *Energy Storage Mater.* **2018**, 11, 16.
- [162] L. Luo, A. Manthiram, *Energy Technol.* **2020**, 8, 2000348.
- [163] L. Chen, Z. Huang, R. Shahbazian Yassar, J. A. Libera, K. C. Klavetter, K. R. Zavadil, J. W. Elam, *ACS Appl. Mater. Interfaces* **2018**, 10, 7043.
- [164] A. Kozen, C. Lin, A. Pearse, M. Schroeder, X. Han, L. Hu, S. Lee, G. Rubloff, M. Noked, *ACS Nano* **2015**, 9, 5884.
- [165] Y. Zhao, D. Wang, Y. Gao, T. Chen, Q. Huang, D. Wang, *Nano Energy* **2019**, 64, 103893.
- [166] M. Li, X. Li, V. Tung, Y. Li, Z. Lai, *ACS Appl. Energy Mater.* **2020**, 3, 2510.
- [167] Y. Liu, Y.-K. Tzeng, D. Lin, A. Pei, H. Lu, N. A. Melosh, Z.-X. Shen, S. Chu, Y. Cui, *Joule* **2018**, 2, 1595.
- [168] C. Zhang, Q. Lan, Y. Liu, J. Wu, H. Shao, H. Zhan, Y. Yang, *Electrochim. Acta* **2019**, 306, 407.
- [169] Z. Wang, Y. Wang, Z. Zhang, X. Chen, W. Lie, Y. B. He, Z. Zhou, G. Xia, Z. Guo, *Adv. Funct. Mater.* **2020**, 30, 2002414.
- [170] Q. Jin, X. Zhang, H. Gao, L. Li, Z. Zhang, *J. Mater. Chem. A* **2020**, 8, 8979.
- [171] H. Li, D. Chao, B. Chen, X. Chen, C. Chuah, Y. Tang, Y. Jiao, M. Jaroeniec, S. Z. Qiao, *J. Am. Chem. Soc.* **2012**, 2020, 142.
- [172] Z. Zhao, J. Wang, M. Cheng, J. Wu, Q. Zhang, X. Liu, C. Wang, J. Wang, K. Li, J. Wang, *Electrochim. Acta* **2020**, 349, 136231.
- [173] R. Zhang, X. Chen, X. Shen, X.-Q. Zhang, X. R. Chen, X.-B. Cheng, C. Yan, C.-Z. Zhao, Q. Zhang, *Joule* **2018**, 2, 764.
- [174] P. Shi, T. Li, R. Zhang, X. Shen, X. B. Cheng, R. Xu, J. Q. Huang, X. R. Chen, H. Liu, Q. Zhang, *Adv. Mater.* **2019**, 31, 1807131.
- [175] Y. Wei, B. Wang, Y. Zhang, M. Zhang, Q. Wang, Y. Zhang, H. Wu, *Adv. Funct. Mater.* **2021**, 31, 2006033.
- [176] Z. A. Ghazi, L. Zhu, H. Wang, A. Naeem, A. M. Khattak, B. Liang, N. A. Khan, Z. Wei, L. Li, Z. Tang, *Adv. Energy Mater.* **2016**, 6, 1601250.
- [177] H. Wang, D. Lin, J. Xie, Y. Liu, H. Chen, Y. Li, J. Xu, G. Zhou, Z. Zhang, A. Pei, Y. Zhu, K. Liu, K. Wang, Y. Cui, *Adv. Energy Mater.* **2019**, 9, 1802720.
- [178] C. Jin, O. Sheng, J. Luo, H. Yuan, C. Fang, W. Zhang, H. Huang, Y. Gan, Y. Xia, C. Liang, *Nano Energy* **2017**, 37, 177.
- [179] C. Jin, O. Sheng, W. Zhang, J. Luo, H. Yuan, T. Yang, H. Huang, Y. Gan, Y. Xia, C. Liang, *Energy Storage Mater.* **2018**, 15, 218.
- [180] Y. Wei, Y. Wang, X. Zhang, B. Wang, Q. Wang, N. Wu, Y. Zhang, H. Wu, *ACS Appl. Mater. Interfaces* **2020**, 12, 35058.
- [181] M. Zhang, Y. Guo, Y. Wei, B. Wang, Y. Zhang, H. Wu, X. Zhou, Y. Zhang, Q. Wang, *J. Mater. Chem. A* **2020**, 8, 18987.
- [182] C.-Y. Wang, Z.-J. Zheng, Y.-Q. Feng, H. Ye, F.-F. Cao, Z.-P. Guo, *Nano Energy* **2020**, 74, 104817.
- [183] J. He, A. Manthiram, *Adv. Energy Mater.* **2020**, 10, 2002654.
- [184] S. Lin, Y. Yan, Z. Cai, L. Liu, X. Hu, *Small* **2018**, 14, 1800616.
- [185] Z. Dai, M. Wang, Y. Zhang, B. Wang, H. Luo, X. Zhang, Q. Wang, Y. Zhang, H. Wu, *Chemistry* **2020**, 26, 8784.
- [186] J. He, A. Manthiram, *Adv. Energy Mater.* **2020**, 10, 1903241.
- [187] L. Kong, H.-J. Peng, J.-Q. Huang, Q. Zhang, *Nano Res.* **2017**, 10, 4027.
- [188] S. Jin, S. Xin, L. Wang, Z. Du, L. Cao, J. Chen, X. Kong, M. Gong, J. Lu, Y. Zhu, H. Ji, R. S. Ruoff, *Adv. Mater.* **2016**, 28, 9094.
- [189] K. Lin, X. Qin, M. Liu, X. Xu, G. Liang, J. Wu, F. Kang, G. Chen, B. Li, *Adv. Funct. Mater.* **2019**, 29, 1903229.
- [190] Y. Ma, B. Yao, M. Zhang, H. Bai, G. Shi, *J. Mater. Chem. A* **2018**, 6, 15603.
- [191] H. Wu, Y. Zhang, Y. Deng, Z. Huang, C. Zhang, Y.-B. He, W. Lv, Q.-H. Yang, *Sci. China Mater.* **2018**, 62, 87.
- [192] Y. Liao, L. Yuan, J. Xiang, W. Zhang, Z. Cheng, B. He, Z. Li, Y. Huang, *Nano Energy* **2020**, 69, 104471.
- [193] T. Liu, J. Hu, C. Li, Y. Wang, *ACS Appl. Energy Mater.* **2019**, 2, 4379.
- [194] Y. Chen, A. Elangovan, D. Zeng, Y. Zhang, H. Ke, J. Li, Y. Sun, H. Cheng, *Adv. Funct. Mater.* **2019**, 30, 1906444.
- [195] Q. Li, S. Zhu, Y. Lu, *Adv. Funct. Mater.* **2017**, 27, 1606422.
- [196] X. Zhang, A. Wang, R. Lv, J. Luo, *Energy Storage Mater.* **2019**, 18, 199.
- [197] C. P. Yang, Y. X. Yin, S. F. Zhang, N. W. Li, Y. G. Guo, *Nat. Commun.* **2015**, 6, 8058.
- [198] Y. An, H. Fei, G. Zeng, X. Xu, L. Ci, B. Xi, S. Xiong, J. Feng, Y. Qian, *Nano Energy* **2018**, 47, 503.
- [199] J. Zhao, G. Zhou, K. Yan, J. Xie, Y. Li, L. Liao, Y. Jin, K. Liu, P. C. Hsu, J. Wang, H. M. Cheng, Y. Cui, *Nat. Nanotechnol.* **2017**, 12, 993.
- [200] X. Zhang, W. Wang, A. Wang, Y. Huang, K. Yuan, Z. Yu, J. Qiu, Y. Yang, *J. Mater. Chem. A* **2014**, 2, 11660.
- [201] T. Chen, W. Kong, P. Zhao, H. Lin, Y. Hu, R. Chen, W. Yan, Z. Jin, *Chem. Mater.* **2019**, 31, 7565.
- [202] H. Kim, J. T. Lee, D.-C. Lee, M. Oschatz, W. I. Cho, S. Kaskel, G. Yushin, *Electrochem. Commun.* **2013**, 36, 38.
- [203] L. L. Kong, L. Wang, Z. C. Ni, S. Liu, G. R. Li, X. P. Gao, *Adv. Funct. Mater.* **2019**, 29, 1808756.
- [204] B. Liu, Y. Zhang, Z. Wang, C. Ai, S. Liu, P. Liu, Y. Zhong, S. Lin, S. Deng, Q. Liu, G. Pan, X. Wang, X. Xia, J. Tu, *Adv. Mater.* **2020**, 32, 2003657.
- [205] Y. X. Ren, L. Zeng, H. R. Jiang, W. Q. Ruan, Q. Chen, T. S. Zhao, *Nat. Commun.* **2019**, 10, 3249.
- [206] L. Ma, M. S. Kim, L. A. Archer, *Chem. Mater.* **2017**, 29, 4181.
- [207] N. Deng, W. Kang, Y. Liu, J. Ju, D. Wu, L. Li, B. S. Hassan, B. Cheng, *J. Power Sources* **2016**, 331, 132.
- [208] B. Liu, X. Wu, S. Wang, Z. Tang, Q. Yang, G. H. Hu, C. Xiong, *Nanomaterials* **2017**, 7, 196.
- [209] H. Yao, K. Yan, W. Li, G. Zheng, D. Kong, Z. W. Seh, V. K. Narasimhan, Z. Liang, Y. Cui, *Energy Environ. Sci.* **2014**, 7, 3381.
- [210] H. Lu, J. Wang, T. Li, H. Du, D. Yi, J. Fang, B. Hong, *J. Solid State Electrochem.* **2017**, 22, 953.
- [211] C. Deng, Z. Wang, S. Wang, J. Yu, D. J. Martin, A. K. Nanjundan, Y. Yamauchi, *ACS Appl. Mater. Interfaces* **2019**, 11, 541.
- [212] Z. A. Ghazi, X. He, A. M. Khattak, N. A. Khan, B. Liang, A. Iqbal, J. Wang, H. Sin, L. Li, Z. Tang, *Adv. Mater.* **2017**, 29, 1606817.
- [213] H. Yuan, J.-Q. Huang, H.-J. Peng, M.-M. Titirici, R. Xiang, R. Chen, Q. Liu, Q. Zhang, *Adv. Energy Mater.* **2018**, 8, 1802107.
- [214] J. Liu, Q. Zhang, Y.-K. Sun, *J. Power Sources* **2018**, 396, 19.
- [215] W. Chen, T. Lei, T. Qian, W. Lv, W. He, C. Wu, X. Liu, J. Liu, B. Chen, C. Yan, J. Xiong, *Adv. Energy Mater.* **2018**, 8, 1702889.
- [216] B. Jin, Y. Li, J. Qian, X. Zhan, Q. Zhang, *ChemElectroChem* **2020**, 7, 4158.
- [217] Q. Wang, N. Yan, M. Wang, C. Qu, X. Yang, H. Zhang, X. Li, H. Zhang, *ACS Appl. Mater. Interfaces* **2015**, 7, 25002.

- [218] F. Chen, H. Li, T. Chen, Z. Chen, Y. Zhang, X. Fan, L. Zhan, L. Ma, X. Zhou, *Colloids Surf. A Physicochem. Eng. Asp.* **2021**, 611, 125870.
- [219] J. Wang, Z. Yao, C. W. Monroe, J. Yang, Y. Nuli, *Adv. Funct. Mater.* **2013**, 23, 1194.
- [220] H. Zhang, X. Hu, Y. Zhang, S. Wang, F. Xin, X. Chen, D. Yu, *Energy Storage Mater.* **2019**, 17, 293.
- [221] B. Jin, L. Yang, J. Zhang, Y. Cai, J. Zhu, J. Lu, Y. Hou, Q. He, H. Xing, X. Zhan, F. Chen, Q. Zhang, *Adv. Energy Mater.* **2019**, 9, 1902938.
- [222] S. H. Chung, A. Manthiram, *Adv. Mater.* **2019**, 31, 1901125.
- [223] A. Fotouhi, D. Auger, L. O'Neill, T. Cleaver, S. Walus, *Energies* **1937**, 2017, 10.
- [224] K. Zhu, C. Wang, Z. Chi, F. Ke, Y. Yang, A. Wang, W. Wang, L. Miao, *Front. Energy Res.* **2019**, 7, 123.
- [225] Y. Li, J. G. Shapter, H. Cheng, G. Xu, G. Gao, *Particuology* **2021**, 58, 1.
- [226] H.-S. Kang, E. Park, J.-Y. Hwang, H. Kim, D. Aurbach, A. Rosenman, Y.-K. Sun, *Adv. Mater. Technol.* **2016**, 1, 1600052.
- [227] X.-B. Cheng, C. Yan, J.-Q. Huang, P. Li, L. Zhu, L. Zhao, Y. Zhang, W. Zhu, S.-T. Yang, Q. Zhang, *Energy Storage Mater.* **2017**, 6, 18.
- [228] S. Waluś, G. Offer, I. Hunt, Y. Patel, T. Stockley, J. Williams, R. Purkayastha, *Energy Storage Mater.* **2018**, 10, 233.
- [229] H. Bao, Y. Dong, X. Wu, G. Li, F. Zhu, W. Guan, X. Wang, Z. Su, *ACS Appl. Mater. Interfaces* **2020**, 12, 36220.
- [230] X. Huang, J. Xue, M. Xiao, S. Wang, Y. Li, S. Zhang, Y. Meng, *Energy Storage Mater.* **2020**, 30, 87.
- [231] M. Zhao, B.-Q. Li, X. Chen, J. Xie, H. Yuan, J.-Q. Huang, *Chem.* **2020**, 6, 3297.
- [232] M. Monisha, P. Permude, A. Ghosh, A. Kumar, S. Zafar, S. Mitra, B. Lochab, *Energy Storage Mater.* **2020**, 29, 350.
- [233] X. Liang, Z. Y. Wen, Y. Liu, M. F. Wu, J. Jin, H. Zhang, X. W. Wu, J. Power Sources **2011**, 196, 9839.
- [234] Z. J. Wang, K. Yang, Y. L. Song, H. Lin, K. Li, Y. H. Cui, L. Y. Yang, F. Pan, *Nano Res.* **2020**, 13, 2431.
- [235] C. Qu, Y. Chen, X. Yang, H. Zhang, X. Li, H. Zhang, *Nano Energy* **2017**, 39, 262.